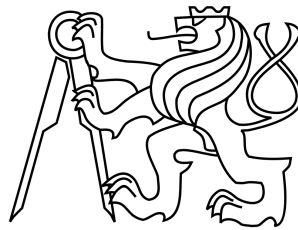


CZECH TECHNICAL UNIVERSITY IN PRAGUE  
FACULTY OF NUCLEAR SCIENCES AND  
PHYSICAL ENGINEERING

DEPARTMENT OF PHYSICS



## DIPLOMA THESIS

Schmidt Modes of Parametric Down-Conversion in  
Non-Linear Waveguide Arrays  
Schmidtovy módy sestupné parametrické frekvenční  
konverze probíhající v soustavě nelineárních  
vlnovodů

**Author:** Pavel Baxant

**Supervisor:** prof. Ing. Igor Jex, DrSc.

**Year:** 2016

## **Prohlášení**

Prohlašuji, že jsem svou diplomovou práci vypracoval samostatně a použil jsem pouze podklady uvedené v příloženém seznamu.

Nemám závažný důvod proti použití tohoto školního díla ve smyslu § 60 zákona č. 121/2000 Sb., o právu autorském, o právech souvisejících s právem autorským a o změně některých zákonů (autorský zákon).

V Praze dne 5. května 2016

.....  
Pavel Baxant

### **Acknowledgements**

I would like to express my gratitude to my supervisor, Prof. Igor Jex, for an interesting topic, support, and especially for his patience.

Next, I would like to thank Aurél Gabris, Ph.D., and Craig Hamilton, Ph.D., for provided consultations and their friendly attitude.

Last but not least, I would like to thank my family.



*Název práce:*

**Schmidtovy módy sestupné parametrické frekvenční konverze probíhající v soustavě nelineárních vlnovodů**

*Autor:* Pavel Baxant

*Obor:* Matematická fyzika

*Druh práce:* Diplomová práce

*Vedoucí práce:* prof. Ing. Igor Jex, DrSc.

Katedra fyziky, Fakulta jaderná a fyzikálně inženýrská,  
České vysoké učení technické v Praze

*Konzultanti:* Aurél Gabris, Ph.D.

Craig Hamilton, Ph.D.

Katedra fyziky, Fakulta jaderná a fyzikálně inženýrská,  
České vysoké učení technické v Praze

*Abstrakt:* Práce se zabývá teoretickým studiem sestupné parametrické frekvenční konverze probíhající v soustavě nelineárních vlnovodů. Hlavním cílem práce je nalezení Schmidtových módů příslušných tomuto procesu. Nejprve odvodíme pohybové rovnice a výstupní stavy interakce probíhající v nelineárních krystalech a následně se zaměříme na interakci probíhající v soustavách vlnovodů. Zavádíme pojem kvantové provázání a definujeme Schmidtův rozklad. Uvádíme analytický rozklad dvoufotonových stavů v krystalech, následně s využitím singulárního rozkladu numericky hledáme Schmidtovy módy příslušné interakci v soustavách vlnovodů.

*Klíčová slova:* kvantové provázání, sestupná parametrická frekvenční konverze, soustava nelineárních vlnovodů, Schmidtův rozklad

*Title:*

**Schmidt Modes of Parametric Down-Conversion in Non-Linear Waveguide Arrays**

*Author:* Pavel Baxant

*Abstract:* This work deals with spontaneous parametric down-conversion (SPDC) in an array of non-linear waveguides and its main goal is to find the Schmidt modes of this process. First, we derive equations of motion and output states of the interaction taking part in non-linear crystals and then we turn our attention to interaction in waveguide arrays. We introduce the quantum entanglement and the Schmidt decomposition. We present the analytic decomposition of biphoton states in bulk crystals, followed by numerically obtained Schmidt modes of biphotons in waveguide arrays. To calculate the modes, we employ the singular value decomposition.

*Keywords:* entanglement, spontaneous parametric down-conversion, waveguide array, Schmidt decomposition

# Contents

<b>Introduction</b>	<b>8</b>
<b>1 Non-Linear Processes in Optics</b>	<b>10</b>
1.1 Brief History of Non-linear Optics . . . . .	10
1.2 Tensor of Non-linear Susceptibility and Maxwell's Equations . .	11
1.3 The second-order phenomena . . . . .	12
1.4 Phase-Matching Techniques . . . . .	13
1.5 Quasi-Phase-Matching . . . . .	14
1.6 Spontaneous Parametric Down-Conversion . . . . .	16
<b>2 SPDC in Waveguide Array</b>	<b>22</b>
2.1 Linear Coupled-Mode Theory . . . . .	22
2.2 Hamiltonian of the Interaction and Output States . . . . .	26
<b>3 Schmidt Decomposition</b>	<b>30</b>
3.1 Quantum Entanglement . . . . .	30
3.2 Reduced States and von Neumann Entropy . . . . .	31
3.3 Schmidt Decomposition . . . . .	33
3.4 Schmidt number . . . . .	35
<b>4 Schmidt Modes of SPDC</b>	<b>38</b>
4.1 Schmidt Modes of SPDC in Bulk Crystal . . . . .	38
4.1.1 Decomposition in Cartesian Coordinates . . . . .	38
4.1.2 Decomposition in Polar Coordinates . . . . .	41
4.2 Schmidt Modes of SPDC in Waveguide Array . . . . .	43
<b>5 Numerical Results</b>	<b>49</b>
5.1 Simulation Parameters . . . . .	49
5.2 Calculated Modes . . . . .	51
<b>Summary</b>	<b>56</b>
<b>Bibliography</b>	<b>57</b>

# Introduction

This work concerns with spontaneous parametric down-conversion, representing an important source of quantum entangled photon pairs. Entanglement is a pure quantum phenomenon, with no classical analogy. The strength and attractiveness of quantum computation, quantum cryptography or quantum teleportation is based on entanglement. The successful realisation of protocols in these fields requires therefore reliable and well controllable sources of entangled states, moving the down-conversion into the centre of interest. The need to obtain entangled states seems to be urgent just today when the manufacturing methods of classical computer processors reaches their physical limitations and the so-called Moore's law, predicting the doubling of the number of transistors in a dense integrated circuit every two years, ceases to be valid. Entangled states can also be used to prove experimentally the violation of Bell's inequalities (and therefore verify the validity of quantum theory).

We are dealing with spontaneous parametric down-conversion taking place in an array of non-linear waveguides. This allows the generated photons to access new spatial degrees of freedom, in addition to the spectral ones. The output states are calculated using the first-order perturbation theory, taking into consideration only the biphoton contribution. This approximation is sufficient because the interaction rate is very low and the probability of detection of more than two photons is negligible. In order to characterize these states (and bipartite entangled states in general), it is useful to introduce the concept of Schmidt decomposition, establishing adjoint Schmidt modes. Calculation of the Schmidt modes of parametric down-conversion in waveguide arrays is the main goal of this work.

In the first chapter, we recall the basics of non-linear optics, with emphasis on spontaneous parametric down-conversion in bulk crystals.

Next chapter is dedicated to parametric down-conversion in waveguide arrays. We introduce the coupled-mode theory, describing the propagation of electromagnetic field in an array of adjacent waveguides. This allows us to introduce the mathematical description of the down-converted biphotons in waveguide arrays.

Quantum entanglement is recalled in the third chapter. We mention reduced states and some entanglement measures and we introduce the Schmidt decomposition.

The fourth chapter deals with the Schmidt modes of parametric down-conversion. First, we present the analytic decomposition of biphoton states in bulk crystals, followed by numerically obtained Schmidt modes of parametric down-conversion in waveguide arrays. To calculate the modes, we decompose the state in an orthonormal basis. We truncate the decomposition, assuming sufficient decrease of proportion of higher modes and then we employ the singular value decomposition algorithm.

Finally, in the last chapter, the modes calculated for three particular cases are presented.

# Chapter 1

## Non-Linear Processes in Optics

### 1.1 Brief History of Non-linear Optics

First, we outline a short history of non-linear optics (inspired by [1]). The first mentions of non-linear optics dates back to the year 1941 when American chemist Gilbert N. Lewis observed non-linear saturation of fluorescence intensity of fluorescein in boric glass with increasing power of excitation.

Real formation of non-linear optics came up with the discovery of the coherent source of light, i.e. with the construction of laser in 1960. Already in 1961, Peter A. Franken discovered second harmonic generation, by focusing the ruby laser with a wavelength 694.2 nm into a quartz sample. At the output of the crystal, there was light observed at 347.1 nm (for this purpose the spectrum of the outgoing light was recorded on photographic paper and the editor of Physical Review Letters mistook the dim spot at 347.1 nm on the photographic paper as a speck of dirt and removed it from the publication). It has also been the first experimental demonstration of conversion of coherent radiation into coherent radiation.

In the 1960s many other discoveries were made, notably sum-frequency generation (1962), the third harmonic generation (1962), electro-optic rectification (1962), difference-frequency generation (1963), optical parametric amplification and generation (1965). These experiments have confirmed theories of non-linear polarization and interaction of waves in non-linear media and provided new methods to generation of coherent radiation.

Another direction of the development of the non-linear optics represented scattering processes. In 1962, Eric J. Woodbury and Wee K. Ng observed stimulated Raman scattering. This discovery had great value because it was the first studied scattering process which was not spontaneous, and in addition, it was possible to use it as a source of coherent light. In 1964, stimulated Brillouin scattering was experimentally observed.

In the 1970s, there were three main areas of new discoveries. The first one was dedicated to new non-linear spectroscopic techniques (coherent anti-Stokes Raman spectroscopy, Doppler-free saturation spectroscopy and laser polariza-

tion spectroscopy). The second one was dedicated to optical phase conjugation, namely the phase conjugation generated by Brillouin scattering (1972) and conjugation generated by three-wave and four-wave interaction (1976-1977). The last studied area concerned optical bistability and hysteresis.

Spontaneous parametric down-conversion (SPDC), which is in the centre of interest of this work, has been first observed by D. C. Burnham and D. L. Weinberg in 1970 [2]. In late 1980s, two independent groups of researchers (Carroll Alley and Yanhua Shih, and Rupamanjari Ghosh and Leonard Mandel) applied SPDC in experiments related to coherence. Today, SPDC is the predominant mechanism for experimentalists to create single photon states. It has also applications in metrology when determining the efficiency of photon detectors and it is one of the major sources of quantum entangled particles.

## 1.2 Tensor of Non-linear Susceptibility and Maxwell's Equations

Non-linear optics offers many interesting phenomena, such as optical harmonic generation, spontaneous parametric down-conversion, frequency conversion, Raman and Brillouin scattering, etc. The origin of all these phenomena lies in the non-linear response of some materials to the incident electromagnetic field.<sup>1</sup> This fact is expressed mathematically by using the tensor of non-linear susceptibility and with its use we may expand the vector of electric polarization in a power series of the field

$$\begin{aligned} \mathbf{P}(\omega_i) = & \chi^{(1)}(\omega_i) \cdot \mathbf{E}(\omega_i) + \sum_{j,k} \chi^{(2)}(\omega_i = \omega_j + \omega_k) : \mathbf{E}(\omega_j) \mathbf{E}(\omega_k) \\ & + \sum_{j,k,l} \chi^{(3)}(\omega_i = \omega_j + \omega_k + \omega_l) : \mathbf{E}(\omega_j) \mathbf{E}(\omega_k) \mathbf{E}(\omega_l) + \dots, \end{aligned} \quad (1.1)$$

where  $\chi^{(n)}$  denotes  $n$ -th order susceptibility which is tensor of the order  $n+1$  ( $\chi^{(1)}$  is the linear susceptibility,  $\chi^{(2)}$  is the lowest order non-linear susceptibility, and so on) and  $\mathbf{E}(\omega_i)$  stands for the incident electric field with frequency  $\omega_i$ . The optical non-linearities are small and this fact led to late experimental discovery of non-linear optical phenomena. Using this expansion, we classify the non-linear processes of various orders. In this work we will consider only second-order processes.

Let us derive equations of motion for electric field in non-linear media (following [3, 4]). We start with Maxwell's equations in volume with no free charges and currents (i.e.  $\rho = 0$ ,  $\mathbf{j} = 0$ )

$$\begin{aligned} \nabla \times \mathbf{E} + \frac{\partial \mathbf{B}}{\partial t} &= 0 \\ \nabla \cdot \mathbf{B} &= 0 \end{aligned}$$

---

<sup>1</sup>These materials are typically formed by strongly non-symmetrical molecules.

$$\begin{aligned}\nabla \times \mathbf{H} - \frac{\partial \mathbf{D}}{\partial t} &= 0 \\ \nabla \cdot \mathbf{D} &= 0.\end{aligned}\tag{1.2}$$

Applying the curl operator on the first equation, we are able to derive

$$\nabla \times \nabla \times \mathbf{E} + \varepsilon_0 \mu_0 \frac{\partial^2 \mathbf{E}}{\partial t^2} + \mu_0 \frac{\partial^2 \mathbf{P}}{\partial t^2} = 0,\tag{1.3}$$

where we have employed the relation for electric induction

$$\mathbf{D} = \varepsilon_0 \mathbf{E} + \mathbf{P},\tag{1.4}$$

and relation for magnetic induction (neglecting the magnetization term)

$$\mathbf{B} = \mu_0 \mathbf{H}.\tag{1.5}$$

Using the operational vector identity

$$\nabla \times \nabla \times \mathbf{A} = \nabla (\nabla \cdot \mathbf{A}) - \Delta \mathbf{A},\tag{1.6}$$

we may re-write (1.3) as

$$\Delta \mathbf{E} - \varepsilon_0 \mu_0 \frac{\partial^2 \mathbf{E}}{\partial t^2} = \mu_0 \frac{\partial^2 \mathbf{P}}{\partial t^2} - \frac{1}{\varepsilon_0} \nabla (\nabla \cdot \mathbf{P}).\tag{1.7}$$

For simplicity, we assume a homogeneous medium (i.e.  $\nabla (\nabla \cdot \mathbf{P}) = 0$ ), so we may write the final equation

$$\Delta \mathbf{E} - \varepsilon_0 \mu_0 \frac{\partial^2 \mathbf{E}}{\partial t^2} = \mu_0 \frac{\partial^2 \mathbf{P}}{\partial t^2}.\tag{1.8}$$

From this equation and (1.1) we are able to derive the equations of motion for non-linear optical phenomena of various orders.

### 1.3 The second-order phenomena

Second-order phenomena are characterized by the term  $\chi^{(2)}$  in (1.1). We assume three interacting monochromatic plane waves propagating along the  $z$ -axis

$$\mathbf{E}_i(z, t) = \mathbf{A}_i(z) \exp(i(k_i z - \omega_i t)) + \text{c.c.},\tag{1.9}$$

where  $\mathbf{A}_i(z)$  is the amplitude of the  $i$ -th wave,  $k_i$  and  $\omega_i$  is its wave number and frequency respectively and c.c. stands for complex conjugation. In addition, we assume  $\omega_3 = \omega_1 + \omega_2$ , expressing the energy conservation. Then, according to (1.1), we are able to write the  $i$ -th component of individual polarization waves with frequencies  $\omega_1, \omega_2, \omega_3$  in the following form

$$P_{1i} = \sum_{j,k} \chi_{ijk}^{(2)} A_{2j}^*(z) A_{3k}(z) \exp(i((k_3 - k_2)z - \omega_1 t)) + \text{c.c.},$$

$$\begin{aligned}
P_{2i} &= \sum_{j,k} \chi_{ijk}^{(2)} A_{1j}^*(z) A_{3k}(z) \exp(i((k_3 - k_2)z - \omega_2 t)) + \text{c.c.}, \\
P_{3i} &= \sum_{j,k} \chi_{ijk}^{(2)} A_{1j}(z) A_{2k}(z) \exp(i((k_1 + k_2)z - \omega_3 t)) + \text{c.c.} \quad (1.10)
\end{aligned}$$

Substituting this result in (1.8) and assuming  $k dA_i/dz \gg d^2 A_i/dz^2$ , expressing spatially slowly varying dependence of amplitudes  $A_i$ , we obtain

$$\begin{aligned}
\frac{dA_{1i}}{dz} &= -\frac{i\omega_1}{2} \left(\frac{\mu_0}{\varepsilon_1}\right)^{1/2} \chi_{ijk}^{(2)} A_{3j} A_{2k}^* \exp(i\Delta k z), \\
\frac{dA_{2k}}{dz} &= -\frac{i\omega_2}{2} \left(\frac{\mu_0}{\varepsilon_2}\right)^{1/2} \chi_{kij}^{(2)} A_{1i}^* A_{3j} \exp(i\Delta k z), \\
\frac{dA_{3j}}{dz} &= -\frac{i\omega_3}{2} \left(\frac{\mu_0}{\varepsilon_3}\right)^{1/2} \chi_{jik}^{(2)} A_{1i} A_{2k} \exp(-i\Delta k z), \quad (1.11)
\end{aligned}$$

where  $\omega_i = k_i/(\mu_0 \varepsilon_i)^{1/2}$  and  $\Delta k = k_3 - k_2 - k_1$  is the so-called momentum (or wave vector) mismatch.

These equations describe various second order processes. The case when radiation of frequency  $\omega_3 = \omega_1 + \omega_2$  is generated from sub-frequency radiations is called sum-frequency generation. Generation of radiation of frequency  $\omega_2 = \omega_3 - \omega_1$  from introduced radiation of frequencies  $\omega_3$  and  $\omega_1$  is called frequency down-conversion, whereas frequency up-conversion describes the process when radiations of frequencies  $\omega_1$  and  $\omega_2$  are introduced and radiation of frequency  $\omega_3 = \omega_1 + \omega_2$  is generated. The degenerated case (when  $\omega_1 = \omega_2$ ) describes the second harmonic generation, i.e. the process when the radiation of frequency  $\omega_3 = 2\omega_1$  is generated from radiation of frequency  $\omega_1$ .

For the purpose of this work, the most interesting is splitting of the radiation of the frequency  $\omega_3$  into two radiations with sub frequencies  $\omega_1$  and  $\omega_2$ . If the signal mode 1 is amplified and the idler mode 2 starts from the vacuum fluctuations, we speak of parametric amplification process. If both the modes 1 and 2 start from the vacuum fluctuations, we speak of the parametric down-conversion process (or parametric generation). More detailed description of this process will be given in the following paragraphs.

## 1.4 Phase-Matching Techniques

It immediately follows from (1.11) that for significant rates of generated fields, it is important to fulfil the phase-matching condition  $\Delta k \approx 0$ . But it is often difficult to achieve this condition because the majority of materials exhibits the so-called normal dispersion – an effect when the refractive index is an increasing function of frequency. The perfect phase-matching condition for collinear beams reads

$$\frac{n_1 \omega_1}{c} + \frac{n_2 \omega_2}{c} = \frac{n_3 \omega_3}{c}, \quad (1.12)$$

where  $n_i$  is the refractive index of the wave at frequency  $\omega_i$  and the energy conservation holds

$$\omega_1 + \omega_2 = \omega_3. \quad (1.13)$$

Employing this condition, we may write

$$n_3 = \frac{n_1 \omega_1 + n_2 \omega_2}{\omega_3} \quad (1.14)$$

and it immediately follows

$$\begin{aligned} n_3 - n_2 &= \frac{n_1 \omega_1 - n_2 (\omega_3 - \omega_2)}{\omega_3} \\ &= \frac{n_1 \omega_1 - n_2 \omega_1}{\omega_3} \\ &= (n_1 - n_2) \frac{\omega_1}{\omega_3}. \end{aligned} \quad (1.15)$$

Expecting  $\omega_3 > \omega_2 > \omega_1$ , it follows for normal dispersion that  $n_3 > n_2 > n_1$ , and hence the left-hand side of the last equation must be positive. However, from the same reason the right-hand side must be negative and therefore the equation has no solution.

Of course, it is possible (at least in principle) to achieve the phase-matching using anomalous dispersion<sup>2</sup>, but the most common procedure is to make use of the birefringence of some crystals. Birefringent crystals have two refractive indices, which depend on the polarization of the electromagnetic radiation propagating inside it. The refractive index of the light polarized in the direction perpendicular to the optic axis of the crystal is called ordinary, while the refractive index of the light polarized in the direction of the optic axis is called extraordinary.

The birefringence is used in the following way. The wave with the highest-frequency  $\omega_3 = \omega_1 + \omega_2$  is polarized in the direction that gives it refractive index with the lower value. And for the polarizations of the lower-frequency waves, there are two choices. We recognize type I phase-matching to be the case in which the lower-frequency waves have the same polarization, and type II phase-matching to be the case where the polarizations are orthogonal. To obtain perfect phase-matching, we have two options - angle tuning and temperature tuning. The first one involves precise angular orientation of the crystal with respect to the propagation direction of the incident beam. The second one makes use of the strong temperature-dependency of birefringence of some crystals. Further details can be found in [4].

## 1.5 Quasi-Phase-Matching

For the cases when the classical phase-matching can not be achieved, there is a technique called quasi-phase matching when the crystal is periodically poled.

---

<sup>2</sup>Anomalous dispersion shows decrease in refractive index with increasing frequency, occurring near an absorption feature.

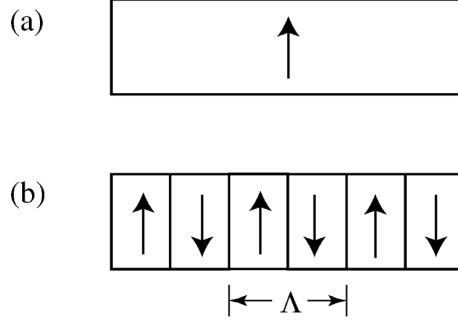


Figure 1.1: Schematic representation of a second-order non-linear optical material in the form of a homogeneous crystal (a) and a periodically poled material (b). Taken from [4]

A periodically poled material is fabricated in such a way that the orientation of one of the crystalline axes is inverted periodically (see Figure 1.1) and this inversion leads also to the inversion of the sign of the non-linear susceptibility tensor  $\chi^{(2)}$ .

Let us denote  $d(z)$  the spatial dependence of the non-linear susceptibility  $\chi^{(2)}(z) = \chi d(z)$ . We expect  $d(z)$  as a square-wave function

$$d(z) = \text{sgn} \left( \cos \left( \frac{2\pi z}{\Lambda} \right) \right), \quad (1.16)$$

where  $\Lambda$  is the poling period. We express  $d(z)$  in the form of a Fourier series

$$d(z) = \sum_{m=-\infty}^{+\infty} G_m \exp(ik_m z), \quad (1.17)$$

where  $k_m = 2\pi m/\Lambda$ . For our case of spatial modulation  $d(z)$  given by (1.16), we have

$$G_m = \frac{2}{m\pi} \sin \left( \frac{m\pi}{2} \right). \quad (1.18)$$

Now we perform the substitution  $\chi_{ijk}^{(2)} \rightarrow \chi_{ijk} G_m \exp(ik_m z)$  in (1.10) and following the same steps as in the previous section, we have

$$\begin{aligned} \frac{dA_{1i}}{dz} &= -\frac{i\omega_1}{2} \left( \frac{\mu_0}{\varepsilon_1} \right)^{1/2} \sum_{j,k} \chi_{ijk} G_m A_{3j} A_{2k}^* \exp [i\Delta k_Q z], \\ \frac{dA_{2k}}{dz} &= -\frac{i\omega_2}{2} \left( \frac{\mu_0}{\varepsilon_2} \right)^{1/2} \sum_{j,k} \chi_{kij} G_m A_{1i}^* A_{3j} \exp [i\Delta k_Q z], \\ \frac{dA_{3j}}{dz} &= -\frac{i\omega_3}{2} \left( \frac{\mu_0}{\varepsilon_3} \right)^{1/2} \sum_{j,k} \chi_{jik} G_m A_{1i} A_{2k} \exp [-i(\Delta k_Q + 2k_m) z], \end{aligned} \quad (1.19)$$

where we have set

$$\Delta k_{QPM} = k_3 - k_1 - k_2 - k_m. \quad (1.20)$$

Because of the tendency for  $G_m$  to decrease with increasing  $m$ , it is most desirable to achieve quasi-phase-matching through use of a first-order interaction  $m = 1$ . Therefore, we have

$$\begin{aligned} \Delta k_{QPM} &= k_3 - k_1 - k_2 - \frac{2\pi}{\Lambda}, \\ G_m &= G_1 = \frac{2}{\pi}. \end{aligned} \quad (1.21)$$

It follows that the optimum poling period is given by

$$\Lambda = \frac{2\pi}{k_3 - k_1 - k_2}. \quad (1.22)$$

## 1.6 Spontaneous Parametric Down-Conversion

Spontaneous parametric down-conversion represents an important second-order non-linear optical process. During this process one photon of the incident field converts into two new subharmonic photons (i.e. with lower frequencies than the incident one). This interaction is mediated by the non-linear crystal, typically LiNbO<sub>3</sub>, KNbO<sub>3</sub>,  $\beta$ -BaB<sub>2</sub>O<sub>4</sub>.<sup>3</sup> The created photons are called signal and idler and they fulfil the phase-matching

$$\begin{aligned} \omega_p &= \omega_s + \omega_i, \\ \mathbf{k}_p &= \mathbf{k}_s + \mathbf{k}_i, \end{aligned} \quad (1.23)$$

where  $\omega_p, \omega_s, \omega_i$  denotes the frequencies of the pump, signal and idler photon and  $\mathbf{k}_p, \mathbf{k}_s, \mathbf{k}_i$  denotes the momenta of these photons. These relations are called phase matching conditions. As we have already mentioned, the process is most effective if these conditions are satisfied.

According to the polarization of the photons, we distinguish two types of spontaneous parametric down-conversion – SPDC type I and SPDC type II. In the first case, the generated photons (signal and idler) have the same polarization – they are polarized ordinary (*o*) and the incident photons are polarized extraordinary (*e*). In the second case, the generated photons have opposite polarizations – signal photons are polarized ordinary and idler photons are polarized extraordinary. The pump photons are still polarized extraordinary. Note that in the first case the generated photons are indistinguishable, unlike the second case. The generated fields in the far field are compared on Figure 1.3.

---

<sup>3</sup>Barium borate BaB<sub>2</sub>O<sub>4</sub> exists in two crystalline forms denoted by  $\alpha$  and  $\beta$ .

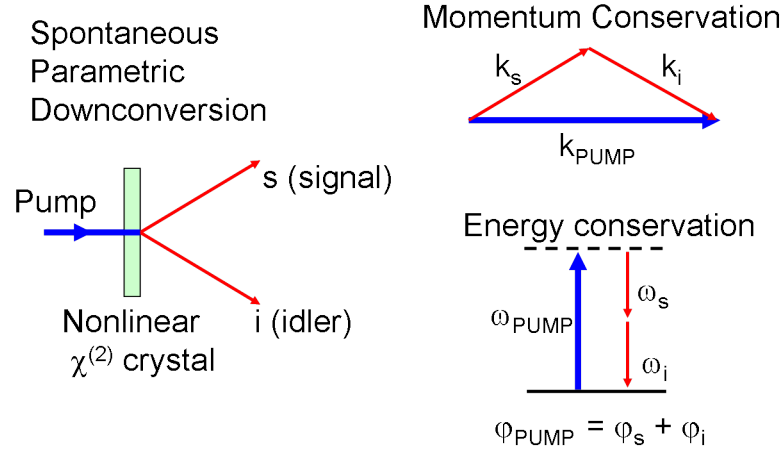


Figure 1.2: Spontaneous parametric down-conversion. On the left we can see the scheme of the interaction. On the right energy and momentum conservation are illustrated. Taken from [2]

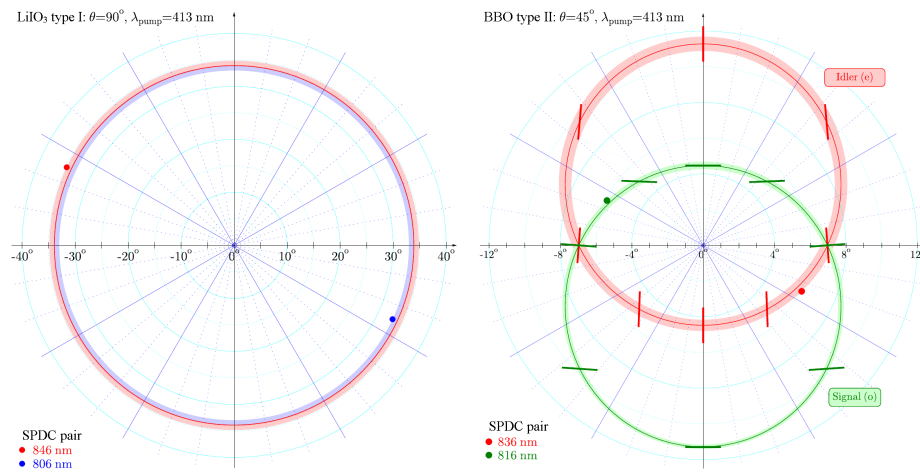


Figure 1.3: Comparison of generated fields far beyond the crystal. On the first picture, we can see SPDC I and on the second one SPDC II. Taken from [5].

Let us introduce the quantum description of the process (following [6–8]). The interaction rate is very low<sup>4</sup>, so we are able to treat the pump field classically (the pump field is almost unchanged when the interaction takes place). The pump field is emitted by laser with a suitably selected wavelength (typically the laser is tuned on the wavelength when the second harmonic generation takes place in the crystal). So, we treat the classical pump field in the form

$$\mathbf{E}(\mathbf{x}, t) = \mathbf{E}^{(+)}(\mathbf{x}, t) + \mathbf{E}^{(-)}(\mathbf{x}, t), \quad (1.24)$$

where

$$\mathbf{E}^{(+)}(\mathbf{x}, t) = i \frac{1}{\mathcal{V}^{1/2}} \sum_{\mathbf{k}, s} \left( \frac{\hbar \omega(\mathbf{k})}{2 \varepsilon_0 n^2(\mathbf{k}, s)} \right)^{1/2} \boldsymbol{\mathcal{E}}_{\mathbf{k}, s} e^{i(\mathbf{k} \cdot \mathbf{x} - \omega t)} \alpha_{\mathbf{k}, s} \quad (1.25)$$

is the positive-frequency part of the incident field and the negative-frequency part is given as a complex conjugate

$$\mathbf{E}^{(-)}(\mathbf{x}, t) = \mathbf{E}^{(+)*}(\mathbf{x}, t). \quad (1.26)$$

The  $\mathcal{V}$  stands for the quantization volume,  $\mathbf{k}$  is the wave vector,  $\omega$  is the frequency,  $s$  denotes the polarization,  $n(\mathbf{k}, s)$  is the refractive index,  $\alpha_{\mathbf{k}, s}$  is the mode amplitude and  $\boldsymbol{\mathcal{E}}_{\mathbf{k}, s}$  is the unit polarization vector satisfying

$$\begin{aligned} \mathbf{k} \cdot \boldsymbol{\mathcal{E}}_{\mathbf{k}, s} &= 0, \\ \boldsymbol{\mathcal{E}}_{\mathbf{k}, s}^* \cdot \boldsymbol{\mathcal{E}}_{\mathbf{k}, s'} &= \delta_{ss'}, \\ \boldsymbol{\mathcal{E}}_{\mathbf{k}, 1} \times \boldsymbol{\mathcal{E}}_{\mathbf{k}, 2} &= \frac{\mathbf{k}}{k}. \end{aligned} \quad (1.27)$$

The generated quantum fields are also divided into the positive-frequency and negative-frequency parts

$$\hat{\mathbf{E}}(\mathbf{x}, t) = \hat{\mathbf{E}}^{(+)}(\mathbf{x}, t) + \hat{\mathbf{E}}^{(-)}(\mathbf{x}, t). \quad (1.28)$$

The positive-frequency part is given by

$$\hat{\mathbf{E}}^{(+)}(\mathbf{x}, t) = i \frac{1}{\mathcal{V}^{1/2}} \sum_{\mathbf{k}, s} \left( \frac{\hbar \omega(\mathbf{k})}{2 \varepsilon_0 n^2(\mathbf{k}, s)} \right)^{1/2} \boldsymbol{\mathcal{E}}_{\mathbf{k}, s} e^{i(\mathbf{k} \cdot \mathbf{x} - \omega t)} \hat{a}_{\mathbf{k}, s}, \quad (1.29)$$

where all quantities are defined in the same manner as in the previous case and  $\hat{a}_{\mathbf{k}, s}$  stands for the annihilation operator of a photon with wave vector  $\mathbf{k}$  and polarization  $s$ . The Hermitian conjugate of the annihilation operator is the creation operator  $\hat{a}_{\mathbf{k}, s}^\dagger$ . These operators satisfy the following commutation relations

---

<sup>4</sup>According to [2], the interaction rate is on the order of one pair per every  $10^{12}$  incoming photons.

$$\begin{aligned}
\left[ \hat{a}_{\mathbf{k}s}, \hat{a}_{\mathbf{k}'s'}^\dagger \right] &= \delta_{\mathbf{k}\mathbf{k}'}^{(3)} \delta_{ss'}, \\
\left[ \hat{a}_{\mathbf{k}s}, \hat{a}_{\mathbf{k}'s'} \right] &= 0, \\
\left[ \hat{a}_{\mathbf{k}s}^\dagger, \hat{a}_{\mathbf{k}'s'}^\dagger \right] &= 0.
\end{aligned} \tag{1.30}$$

The negative-frequency part of the generated field is given as Hermitian conjugate of the positive-frequency part

$$\hat{\mathbf{E}}^{(-)}(\mathbf{x}, t) = \hat{\mathbf{E}}^{(+)\dagger}(\mathbf{x}, t) \tag{1.31}$$

We consider a crystal as a rectangular parallelepiped of sides  $l_1, l_2, l_3$  (and volume  $V = l_1 l_2 l_3$ ) with a centre placed at the origin. We assume that the crystal is embedded in a passive medium of the same refractive index to avoid complications with refraction at the interface. The interaction Hamiltonian is then given as

$$\hat{H}_I(t) = \int_V \chi_{lij}^{(2)} E_i^{(+)}(\mathbf{x}, t) \hat{E}_i^{(-)}(\mathbf{x}, t) \hat{E}_j^{(-)}(\mathbf{x}, t) d^3x + \text{h.c.}, \tag{1.32}$$

where h.c. stands for the Hermitian conjugate. Substituting for the fields, we obtain

$$\begin{aligned}
\hat{H}_I(t) &= \frac{1}{\mathcal{V}^{3/2}} \sum_{\mathbf{k}_p, s_p} \sum_{\mathbf{k}_s, s_s} \sum_{\mathbf{k}_i, s_i} \chi_{lij}^{(2)}(\omega_p, \omega_s, \omega_i) (\boldsymbol{\mathcal{E}}_{\mathbf{k}_p, s_p})_l (\boldsymbol{\mathcal{E}}_{\mathbf{k}_s, s_s}^*)_i (\boldsymbol{\mathcal{E}}_{\mathbf{k}_i, s_i}^*)_j \\
&\times g_{\mathbf{k}_p, s_p} g_{\mathbf{k}_s, s_s}^* g_{\mathbf{k}_i, s_i}^* e^{i(\omega_s + \omega_i - \omega_p)t} \\
&\times \int_V e^{i(\mathbf{k}_p - \mathbf{k}_s - \mathbf{k}_i) \cdot \mathbf{x}} \alpha_{\mathbf{k}_p, s_p} \hat{a}_{\mathbf{k}_s, s_s} \hat{a}_{\mathbf{k}_i, s_i}^\dagger d^3x + \text{h.c.},
\end{aligned} \tag{1.33}$$

where we have set

$$g_{\mathbf{k}, s} = i \left( \frac{\hbar \omega(\mathbf{k})}{2\varepsilon_0 n^2(\mathbf{k}, s)} \right)^{1/2}. \tag{1.34}$$

The interaction Hamiltonian can be used to write the state of the field in the form

$$|\psi(t)\rangle = \exp \left[ -\frac{i}{\hbar} \int_0^t \hat{H}(t') dt' \right] |0\rangle, \tag{1.35}$$

where  $|0\rangle$  is the initial state (i.e. in the time  $t = 0$  the signal and idler field are in vacuum state). To first order in time, we can write

$$|\psi(t)\rangle \approx |0\rangle - \frac{i}{\hbar} \frac{Vt}{\mathcal{V}^{3/2}} \sum_{\mathbf{k}_p, s_p} \sum_{\mathbf{k}_s, s_s} \sum_{\mathbf{k}_i, s_i} \chi_{lij}^{(2)}(\omega_p, \omega_s, \omega_i) (\boldsymbol{\mathcal{E}}_{\mathbf{k}_p, s_p})_l (\boldsymbol{\mathcal{E}}_{\mathbf{k}_s, s_s}^*)_i (\boldsymbol{\mathcal{E}}_{\mathbf{k}_i, s_i}^*)_j$$

$$\begin{aligned}
& \times \operatorname{sinc}\left(\frac{1}{2}(\omega_s + \omega_i - \omega_p)t\right) e^{\frac{i}{2}(\omega_s + \omega_i - \omega_p)t} \\
& \times \left[ \prod_{m=1}^3 \operatorname{sinc}\left(\frac{1}{2}(\mathbf{k}_p - \mathbf{k}_s - \mathbf{k}_i)_m l_m\right) \right] \alpha_{\mathbf{k}_p, s_p} \hat{a}_{\mathbf{k}_s, s_s}^\dagger \hat{a}_{\mathbf{k}_i, s_i}^\dagger |0\rangle, \quad (1.36)
\end{aligned}$$

where  $\operatorname{sinc}(x) = \sin x/x$ .

Now, we make some simplifying assumptions (details can be found in [8–10]):

1. We expect the interaction time long enough, so that the term  $\operatorname{sinc}\left(\frac{1}{2}(\omega_s + \omega_i - \omega_p)t\right)$  is significant only when  $\omega_p = \omega_s + \omega_i$ .
2. The pump beam propagates along the  $z$ -axis and the crystal is large enough in the  $x$  and  $y$  directions to allow to extend  $l_x$  and  $l_y$  to infinity. Then we can make the following replacement

$$\begin{aligned}
\prod_{m=1}^3 \operatorname{sinc}\left(\frac{1}{2}(\mathbf{k}_p - \mathbf{k}_s - \mathbf{k}_i)_m l_m\right) &= \delta(\mathbf{q}_p - \mathbf{q}_s - \mathbf{q}_i) \\
&\times \operatorname{sinc}((\mathbf{k}_p - \mathbf{k}_s - \mathbf{k}_i)_z L), \quad (1.37)
\end{aligned}$$

where  $\mathbf{q}_j = (k_{jx}, k_{jy})$  is the transverse  $xy$ -component of  $\mathbf{k}_j$  and  $L = l_z$  is the thickness of the crystal.

3. The terms  $g_{\mathbf{k}, s}$  and  $\chi_{lij}^{(2)}$  are slowly-varying functions of  $\mathbf{k}$ , so that they may be taken as constants and removed from integrals.
4. The quantization volume is large enough to allow us to replace the summations over momenta  $\mathbf{k}$  by integrals.
5. We choose only one polarization of each photon to avoid the summations over  $s$ .

These simplifications lead us to the expression

$$|\psi(t)\rangle \approx |0\rangle + \mathcal{C} \int d^3 k_s \int d^3 k_i \Phi(\mathbf{q}_s, \mathbf{q}_i) \hat{a}^\dagger(\mathbf{k}_s) \hat{a}^\dagger(\mathbf{k}_i) |0\rangle, \quad (1.38)$$

where  $\mathcal{C}$  contains all constants and  $\Phi(\mathbf{q}_s, \mathbf{q}_i)$  is the so-called phase-matching function

$$\Phi(\mathbf{q}_s, \mathbf{q}_i) = \alpha(\mathbf{q}_s + \mathbf{q}_i) \operatorname{sinc}((\mathbf{k}_p - \mathbf{k}_s - \mathbf{k}_i)_z L). \quad (1.39)$$

Finally, we use the collinear approximation [9]. We assume the pump beam having a narrow angular spectrum and the generated modes being observed only in points close to the  $z$ -axis, so that  $|\mathbf{q}| \ll |\mathbf{k}|$  holds for all three modes. Under these conditions we may write

$$(\mathbf{k}_p - \mathbf{k}_s - \mathbf{k}_i)_z = \sqrt{k_p^2 - q_p^2} - \sqrt{k_s^2 - q_s^2} - \sqrt{k_i^2 - q_i^2}$$

$$\approx k_p \left( 1 - \frac{q_p^2}{2k_p^2} \right) - k_s \left( 1 - \frac{q_s^2}{2k_s^2} \right) - k_i \left( 1 - \frac{q_i^2}{2k_i^2} \right), \quad (1.40)$$

where we have employed the Taylor expansion up to the first order, assuming  $q \ll k$ . For the near-degenerate case [10], we have  $k_s \approx k_i \approx k_p/2$ , leading to

$$(\mathbf{k}_p - \mathbf{k}_s - \mathbf{k}_i)_z \approx \frac{|\mathbf{q}_s - \mathbf{q}_i|^2}{2k_p}, \quad (1.41)$$

where we have used

$$q_p = |\mathbf{q}_s + \mathbf{q}_i|. \quad (1.42)$$

The overall result for the phase-matching function then reads

$$\Phi(\mathbf{q}_s, \mathbf{q}_i) = \alpha(\mathbf{q}_s + \mathbf{q}_i) \text{sinc} \left( \frac{|\mathbf{q}_s - \mathbf{q}_i|^2}{2k_p} L \right), \quad (1.43)$$

and we use it in the fourth chapter to find the Schmidt modes.

After presenting the basics for non-linear processes with particular emphasis on parametric down-conversion, we turn our attention to optical waveguide arrays.

## Chapter 2

# SPDC in Waveguide Array

In this chapter we will present the description of spontaneous parametric down-conversion taking part in an array of quadratic non-linear waveguides. In order to proceed with this task, we have to introduce the linear coupled-mode theory, describing the propagation of electromagnetic field in the waveguide array.

### 2.1 Linear Coupled-Mode Theory

First, we derive equations of motion describing the propagation of electromagnetic fields in an array of adjacent waveguides (following [11, 12]). The waveguides are mathematically represented as a small modification of refractive index  $n_0$ . We start from the equation (1.8)

$$\Delta \mathbf{E} - \varepsilon_0 \mu_0 \frac{\partial^2 \mathbf{E}}{\partial t^2} = \mu_0 \frac{\partial^2 \mathbf{P}}{\partial t^2}. \quad (2.1)$$

We expect just the linear contribution of polarization  $\mathbf{P} = \mathbf{P}^{(1)}$ , so we may employ the following relation

$$\mathbf{D} = \varepsilon_0 \mathbf{E} + \mathbf{P} = \varepsilon_0 \varepsilon \mathbf{E}, \quad (2.2)$$

where  $\varepsilon = n^2$  is the relative permittivity. This assumption allows us to write

$$\Delta \mathbf{E}(\mathbf{x}, t) - \frac{n^2(\mathbf{x})}{c^2} \frac{\partial^2 \mathbf{E}}{\partial t^2} = 0. \quad (2.3)$$

Let the waveguides be oriented in such a way that the electromagnetic field propagates along the  $z$  direction. The waveguides are fabricated by modifying the refractive index of a homogeneous, isotropic slab along the  $x$  and  $y$  direction. Let us denote by  $n_j(x, y) = n_0 + \delta n_j(x, y)$  the refractive index distribution for the  $j$ -th waveguide, with  $n_0$  the unmodulated refractive index of the bulk and  $\delta n_j \ll n_0$  the localized perturbation at the position of the  $j$ -th waveguide. The refractive index of the whole structure is then given by

$$n(x, y) = n_0 + \sum_{j=1}^N \delta n_j(x, y) \quad (2.4)$$

and its square

$$n^2(x, y) \approx n_0^2 + 2 \sum_{j=1}^N n_0 \delta n_j(x, y) = n_0^2 + \sum_{j=1}^N \Delta n_j^2(x, y). \quad (2.5)$$

Here we have neglected the terms  $\delta n_j(x, y) \delta n_k(x, y)$  and we have set  $\Delta n_j^2(x, y) = 2n_0 \delta n_j(x, y)$ , assuming

$$\Delta n_j^2(x, y) = \begin{cases} n_j^2(x, y) - n_0^2 & \text{inside the } j\text{-th waveguide} \\ 0 & \text{elsewhere.} \end{cases} \quad (2.6)$$

Let us denote  $\mathcal{E}_j(x, y)$  the solution of unperturbed equation for the  $j$ -th isolated waveguide

$$\left( \Delta^\perp + \frac{\omega^2}{c^2} n_j^2(x, y) \right) \mathcal{E}_j(x, y) = \beta_j^2 \mathcal{E}_j(x, y), \quad (2.7)$$

where  $\beta_j$  stands for the corresponding propagation constant and the Laplace operator is restricted just on the  $x$  and  $y$  directions  $\Delta^\perp = \partial^2/\partial x^2 + \partial^2/\partial y^2$ . The corresponding propagating field in the isolated  $j$ -th waveguide is given by

$$\mathbf{E}_j = \mathcal{E}_j(x, y) e^{-i(\omega t - \beta_j z)}. \quad (2.8)$$

We expect that the presence of other waveguides does not affect the transverse modes  $\mathcal{E}_j(x, y)$  of each waveguide and we approximate the total electric field satisfying the wave equation (2.3) in the array by

$$\mathbf{E}(\mathbf{x}, t) = \sum_{j=1}^N A_j(z) \mathcal{E}_j(x, y) e^{-i(\omega t - \beta_j z)} + \text{c.c.}, \quad (2.9)$$

where the mode amplitudes  $A_j(z)$ .

Now, we derive the total power carried by the field at distance  $z$ . It is obtained by integrating the  $z$ -component of the time-averaged Poynting vector  $\mathbf{S} = \frac{1}{2} \text{Re}(\mathbf{E}(\mathbf{x}, t) \times \mathbf{H}^*(\mathbf{x}, t))$  over the cross-sectional area of the medium

$$P(z) = \iint \frac{1}{2} \text{Re}(\mathbf{E}(\mathbf{x}, t) \times \mathbf{H}^*(\mathbf{x}, t)) \cdot \hat{\mathbf{z}} \, dx \, dy, \quad (2.10)$$

where  $\mathbf{H}(\mathbf{x}, t)$  is the magnetic field and  $\hat{\mathbf{z}}$  is a unit vector in the  $z$ -direction. Let us assume that the modes obey to the normalization

$$\alpha_j \iint \mathcal{E}_j(x, y) \cdot \mathcal{E}_j^*(x, y) \, dx \, dy = 1, \quad (2.11)$$

where we have set

$$\alpha_j = \frac{\beta_j}{2\omega\mu_0} = \frac{1}{2} n_j c \varepsilon_0 \approx \frac{1}{2} c n_0 \varepsilon_0. \quad (2.12)$$

Assuming

$$\iint \boldsymbol{\mathcal{E}}_j(x,y) \cdot \boldsymbol{\mathcal{E}}_k^*(x,y) dx dy \ll \iint \boldsymbol{\mathcal{E}}_j(x,y) \cdot \boldsymbol{\mathcal{E}}_j^*(x,y) dx dy, \quad (2.13)$$

we may write

$$(z) \approx \sum_{j=1}^N |A_j(z)|^2 \left( \alpha_j \iint |\boldsymbol{\mathcal{E}}_j(x,y)|^2 dx dy \right) \approx \sum_{j=1}^N |A_j(z)|^2. \quad (2.14)$$

Let the  $k$ -th waveguide is initially excited, then the input power reads

$$P_{\text{peak}} = |A_k(0)|^2. \quad (2.15)$$

We derive the term  $\Delta \mathbf{E}(\mathbf{x}, t)$ . We employ the Fresnel approximation, leading to the omission of second derivatives of mode amplitudes  $\psi_j(z)$  due to their slow change along the  $z$ -direction

$$\begin{aligned} \Delta \mathbf{E}(\mathbf{x}, t) &\approx 2i \sum_{j=1}^N \beta_j \frac{dA_j(z)}{dz} \boldsymbol{\mathcal{E}}_j(x,y) e^{-i(\omega t - \beta_j z)} \\ &\quad + \sum_{j=1}^N A_j(z) \left( \Delta^\perp \boldsymbol{\mathcal{E}}_j(x,y) \right) e^{-i(\omega t - \beta_j z)} \\ &\quad - \sum_{j=1}^N \beta_j^2 A_j(z) \boldsymbol{\mathcal{E}}_j(x,y) e^{-i(\omega t - \beta_j z)} \\ &= 2i \sum_{j=1}^N \beta_j \frac{dA_j(z)}{dz} \boldsymbol{\mathcal{E}}_j(x,y) e^{-i(\omega t - \beta_j z)} \\ &\quad - \frac{\omega^2}{c^2} \sum_{j=1}^N n_j^2(x) A_j(z) \boldsymbol{\mathcal{E}}_j(x,y) e^{-i(\omega t - \beta_j z)} \\ &\approx 2i \sum_{j=1}^N \beta_j \frac{dA_j(z)}{dz} \boldsymbol{\mathcal{E}}_j(x,y) e^{-i(\omega t - \beta_j z)} - \frac{\omega^2}{c^2} n_0^2 \mathbf{E}(\mathbf{x}, t) \\ &\quad - \frac{\omega^2}{c^2} \sum_{j=1}^N \Delta n_j^2(x) A_j(z) \boldsymbol{\mathcal{E}}_j(x,y) e^{-i(\omega t - \beta_j z)}, \end{aligned} \quad (2.16)$$

and we have used (2.7) and (2.6). With the help of (2.3) and (2.5), we obtain

$$\begin{aligned} 2i \sum_{j=1}^N \beta_j \frac{dA_j(z)}{dz} \boldsymbol{\mathcal{E}}_j(x,y) e^{-i(\omega t - \beta_j z)} &\approx \\ &\approx \frac{\omega^2}{c^2} \sum_{j=1}^N \Delta n_j^2(x) \left( \mathbf{E}(\mathbf{x}, t) - A_j(z) \boldsymbol{\mathcal{E}}_j(x,y) e^{i(\omega t - \beta_j z)} \right). \end{aligned} \quad (2.17)$$

We multiply the last equation with  $\mathcal{E}_k^*(x, y)$  and integrate over the  $xy$ -plane, obtaining

$$i \frac{dA_k(z)}{dz} \approx \frac{\omega^2 \alpha_k}{2c^2 \beta_k} \sum_{\substack{l=1 \\ l \neq j}}^N A_l(z) e^{-i(\beta_k - \beta_l)z} \sum_{j=1}^N \iint \Delta n_j^2(x) \mathcal{E}_l(x, y) \cdot \mathcal{E}_k^*(x, y) dx dy, \quad (2.18)$$

where we have used (2.5), (2.11) and (2.13). We assume that the mode distributions and the refractive index perturbations are highly peaked around the centre of the waveguides. Then, we can keep only integrals that involve nearest neighbouring waveguides, which we denote as

$$\begin{aligned} \Omega_k &\approx \frac{\omega \varepsilon_0}{4} \iint \Delta n_{k\pm 1}^2(x) \mathcal{E}_k(x, y) \cdot \mathcal{E}_k^*(x, y) dx dy, \\ C_{k,k\pm 1} &\approx \frac{\omega \varepsilon_0}{4} \iint \Delta n_k^2(x) \mathcal{E}_{k\pm 1}(x, y) \cdot \mathcal{E}_k^*(x, y) dx dy. \end{aligned} \quad (2.19)$$

Now, we can write

$$\begin{aligned} i \frac{dA_k(z)}{dz} &\approx \Omega_k A_k(z) + C_{k,k-1} A_{k-1}(z) e^{-i(\beta_k - \beta_{k-1})z} \\ &\quad + C_{k,k+1} A_{k+1}(z) e^{-i(\beta_k - \beta_{k+1})z}. \end{aligned} \quad (2.20)$$

Setting  $A_k(z) = a_k(z) e^{i\Omega_k z}$  and  $\beta'_k = \beta_k + \Omega_k$ , we have

$$i \frac{da_k(z)}{dz} + C_{k,k-1} a_{k-1}(z) e^{-i(\beta'_k - \beta'_{k-1})z} + C_{k,k+1} a_{k+1}(z) e^{-i(\beta'_k - \beta'_{k+1})z} \approx 0. \quad (2.21)$$

For identical waveguides (i.e.  $\beta'_k = \beta_0$  and  $C_{k,l} = C$ ), these equations are simplified to

$$i \frac{da_k(z)}{dz} + C (a_{k-1}(z) + a_{k+1}(z)) \approx 0. \quad (2.22)$$

We expect the solution in the form of a Bloch wave (details can be found in [12, 13])

$$a_n(z) = a_0 \exp [i(nk_x d + K_z z)]. \quad (2.23)$$

Inserting this ansatz into the last equation we obtain

$$K_z = 2C \cos(k_x d), \quad (2.24)$$

where  $d$  is the distance between individual waveguides and  $k_x$  is the transverse momentum. The quantity  $k_x d$  is called normalized transverse momentum (or normalized Bloch vector) and in the following, it will be denoted by  $k^\perp$ . The final result can be written as

$$\mathbf{E}^{(+)}(\mathbf{x}, t) = \sum_j a_0 \mathcal{E}_j(x, y) e^{-i(\omega t - \beta z)} \quad (2.25)$$

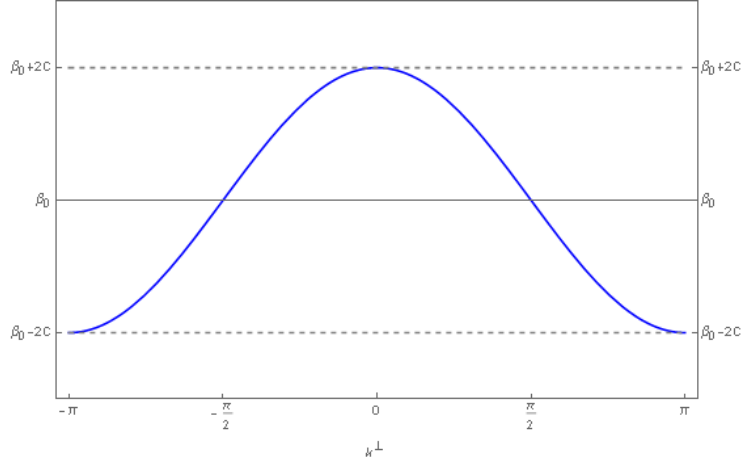


Figure 2.1: Dispersion relation of the Bloch waves in a waveguide array. It is the dependence of the propagation vector  $\beta$  on the normalized transverse momentum  $k^\perp$ .

$$= \sum_j a_j \mathcal{E}_j(x, y) e^{-i(\omega t - (\beta_0 + \Omega + 2C \cos(k^\perp))z)}.$$

So, we have derived the dispersion relation of the waveguide array

$$\beta = \beta_0 + \Omega + 2C \cos(k^\perp). \quad (2.26)$$

Further, we will neglect the term  $\Omega$ , because its contribution is small.

The solution of equation (2.22) can be found using the Fourier transform

$$\tilde{a}(k^\perp, z) = \frac{1}{2\pi} \sum_j a_j(0) e^{-ij k^\perp}. \quad (2.27)$$

The inverse transform is given by

$$a_j(z) = \int_{-\pi}^{\pi} \tilde{a}(k^\perp, z) e^{ijk^\perp} dk^\perp. \quad (2.28)$$

## 2.2 Hamiltonian of the Interaction and Output States

Now, we make use of the results and approaches introduced in the preceding paragraphs to derive the mathematical description of spontaneous parametric down-conversion in an array of non-linear waveguides (following [14, 15]). During this process, the signal and idler photons are generated in the illuminated waveguide and they subsequently spread to the neighbouring waveguides.

As we have derived in the previous section, the dispersion relation between the propagation vector  $\beta$  and the normalized transverse momentum  $k^\perp = k_x d$  in the waveguide array with nearest neighbour coupling is given by

$$\beta(\omega, k^\perp) = \beta^{(0)}(\omega) + 2C(\omega) \cos(k^\perp). \quad (2.29)$$

Employing this relation we are able to express the generated field in the  $n$ -th waveguide as

$$\hat{E}_n^{(+)}(z, t) = \hat{E}_n^{(-)\dagger}(z, t) = B \int_{-\pi}^{\pi} dk^{\perp} \int_{-\infty}^{+\infty} d\omega e^{ik^{\perp}n} e^{i(\beta(\omega, k^{\perp})z - \omega t)} \hat{a}(\omega, k^{\perp}), \quad (2.30)$$

where the term  $B$  collects all constants and  $\hat{a}(\omega, k^{\perp})$  is the annihilation operator of the photon with frequency  $\omega$  and transverse momentum  $k^{\perp}$ . We have also divided the field into the positive (+) and negative (-) frequency parts.

As in the case of the spontaneous parametric conversion in the bulk crystal, the pump field is treated classically

$$\begin{aligned} E_{p,n}^{(+)}(z, t) &= E_{p,n}^{(-)*}(z, t) = \int_{-\infty}^{+\infty} d\omega_p A_n \alpha(\omega_p) e^{i(\beta^{(0)}(\omega_p)z - \omega_p t)} \\ &= \int_{-\pi}^{\pi} dk_p^{\perp} \int_{-\infty}^{+\infty} d\omega_p \tilde{A}(k_p^{\perp}) \alpha(\omega_p) e^{ik_p^{\perp}n} e^{i(\beta^{(0)}(\omega_p)z - \omega_p t)}. \end{aligned} \quad (2.31)$$

Note, that we have used the propagation constant for the isolated waveguide, because we expect that the pump field does not couple to the neighbouring waveguides (due to the frequency dependent coupling parameter  $C(\omega)$  which is for the pump photons small enough). The Bloch mode distribution  $\tilde{A}(k_p^{\perp})$  is given by the Fourier transform

$$\tilde{A}(k_p^{\perp}) = \frac{1}{2\pi} \sum_n A_n e^{-ik_p^{\perp}n}, \quad (2.32)$$

and  $A_n$  is the amplitude of the pump field in the  $n$ -th waveguide.

Now, we may express the interaction Hamiltonian as

$$\hat{H}_I(t) = \chi^{(2)} \int_{-L}^0 dz \sum_n \left( E_{p,n}^{(+)}(z, t) \hat{E}_n^{(-)}(z, t) \hat{E}_n^{(-)}(z, t) + \text{h.c.} \right), \quad (2.33)$$

where  $\chi^{(2)}$  expresses the second-order non-linearity of the material,  $L$  is the length of the individual waveguide and h.c. stands for the hermitian conjugate. We insert (2.30) and (2.31) into the last equation and perform the integration in the  $z$ -coordinate

$$\begin{aligned} \hat{H}_I(t) &= \frac{\varepsilon_0}{2} \int_{-L}^0 dz \sum_n \chi^{(2)} \left[ \int_{-\infty}^{+\infty} d\omega_p A_n \alpha(\omega_p) e^{i(\beta^{(0)}(\omega_p)z - \omega_p t)} \right. \\ &\quad \times B^* \int_{-\pi}^{\pi} dk_s^{\perp} \int_{-\infty}^{+\infty} d\omega_s e^{-ik_s^{\perp}n} e^{-i(\beta(\omega_s, k_s^{\perp})z - \omega_s t)} \hat{a}^{\dagger}(\omega_s, k_s^{\perp}) \\ &\quad \left. \times B^* \int_{-\pi}^{\pi} dk_i^{\perp} \int_{-\infty}^{+\infty} d\omega_i e^{-ik_i^{\perp}n} e^{-i(\beta(\omega_i, k_i^{\perp})z - \omega_i t)} \hat{a}^{\dagger}(\omega_i, k_i^{\perp}) + \text{h.c.} \right] \\ &= \varepsilon_0 \chi^{(2)} L \pi (B^*)^2 \int_{-\infty}^{+\infty} d\omega_p \int_{-\pi}^{\pi} dk_s^{\perp} \int_{-\infty}^{+\infty} d\omega_s \int_{-\pi}^{\pi} dk_i^{\perp} \int_{-\infty}^{+\infty} d\omega_i \end{aligned}$$

$$\left[ \alpha(\omega_p) \tilde{A}(k_s^\perp + k_i^\perp) e^{-i(\omega_p - \omega_s - \omega_i)t} e^{-i\Delta\beta(\omega_p, \omega_s, \omega_i, k_s^\perp, k_i^\perp) \frac{L}{2}} \right. \\ \left. \times \text{sinc} \left( \Delta\beta(\omega_p, \omega_s, \omega_i, k_s^\perp, k_i^\perp) \frac{L}{2} \right) \hat{a}^\dagger(\omega_s, k_s^\perp) \hat{a}^\dagger(\omega_i, k_i^\perp) + \text{h.c.} \right], \quad (2.34)$$

where the subscripts  $p, s, i$  denote the pump, signal and idler photons and we have set

$$\Delta\beta(\omega_p, \omega_s, \omega_i, k_s^\perp, k_i^\perp) = \beta^{(0)}(\omega_p) - \beta(\omega_s, k_s^\perp) - \beta(\omega_i, k_i^\perp).$$

As we have mentioned in the previous chapter, the rate of the down-conversion interaction is very low, thus we may employ the first order perturbation theory

$$|\Psi\rangle \approx |0\rangle - \frac{i}{\hbar} \int_{-\infty}^{+\infty} \hat{H}(t) |0\rangle dt. \quad (2.35)$$

The state is evaluated at a sufficiently long time after the interaction takes place in the array, which allows us to extend the time integration to infinity. The input state was considered to be the vacuum. We are interested just in the biphoton part of the state and therefore we drop the vacuum contribution. After the appropriate renormalization, we may write

$$|\Psi\rangle = \mathcal{N}_0 \int_{-\infty}^{+\infty} \hat{H}(t) |0\rangle dt. \quad (2.36)$$

We perform the time-integration of the Hamiltonian (2.34)

$$\begin{aligned} \mathcal{N}_0 \int_{-\infty}^{+\infty} \hat{H}_I(t) dt &= 2\varepsilon_0 \chi^{(2)} L \pi^2 (B^*)^2 \mathcal{N}_0 \\ &\times \int_{-\infty}^{+\infty} d\omega_p \int_{-\pi}^{\pi} dk_s^\perp \int_{-\infty}^{+\infty} d\omega_s \int_{-\pi}^{\pi} dk_i^\perp \int_{-\infty}^{+\infty} d\omega_i \\ &\alpha(\omega_p) \tilde{A}(k_s^\perp + k_i^\perp) \delta(\omega_p - \omega_s - \omega_i) e^{-i\Delta\beta(\omega_p, \omega_s, \omega_i, k_s^\perp, k_i^\perp) \frac{L}{2}} \\ &\times \text{sinc} \left( \Delta\beta(\omega_p, \omega_s, \omega_i, k_s^\perp, k_i^\perp) \frac{L}{2} \right) \hat{a}^\dagger(\omega_s, k_s^\perp) \hat{a}^\dagger(\omega_i, k_i^\perp) \\ &+ \text{h.c.} \\ &= \int_{-\pi}^{\pi} dk_s^\perp \int_{-\infty}^{+\infty} d\omega_s \int_{-\pi}^{\pi} dk_i^\perp \int_{-\infty}^{+\infty} d\omega_i \\ &\left[ f(\omega_s, \omega_i, k_s^\perp, k_i^\perp) \hat{a}^\dagger(\omega_s, k_s^\perp) \hat{a}^\dagger(\omega_i, k_i^\perp) + \text{h.c.} \right], \quad (2.37) \end{aligned}$$

where  $\delta(x)$  is the Dirac delta function. We have also set

$$\begin{aligned} f(\omega_s, \omega_i, k_s^\perp, k_i^\perp) &= \mathcal{N} \alpha(\omega_p = \omega_s + \omega_i) \tilde{A}(k_s^\perp + k_i^\perp) e^{-i\Delta\beta(\omega_p = \omega_s + \omega_i, \omega_s, \omega_i, k_s^\perp, k_i^\perp) \frac{L}{2}} \\ &\times \text{sinc} \left( \Delta\beta(\omega_p = \omega_s + \omega_i, \omega_s, \omega_i, k_s^\perp, k_i^\perp) \frac{L}{2} \right), \quad (2.38) \end{aligned}$$

where  $\mathcal{N}$  collects all constants and it also guarantees the normalization of the state. For simplicity, we will omit the first argument in the phase mismatch, so in the following text we have

$$\begin{aligned}\Delta\beta(\omega_s, \omega_i, k_s^\perp, k_i^\perp) &= \Delta\beta(\omega_p = \omega_s + \omega_i, \omega_s, \omega_i, k_s^\perp, k_i^\perp) \\ &= \beta^{(0)}(\omega_s + \omega_i) - \beta(\omega_s, k_s^\perp) - \beta(\omega_i, k_i^\perp).\end{aligned}\quad (2.39)$$

Now, it is easy to write the final result

$$\begin{aligned}|\Psi\rangle &= \int_{-\infty}^{+\infty} d\omega_s \int_{-\infty}^{+\infty} d\omega_i \int_{-\pi}^{\pi} dk_s^\perp \int_{-\pi}^{\pi} dk_i^\perp f(\omega_s, \omega_i, k_s^\perp, k_i^\perp) \\ &\quad \times \hat{a}^\dagger(\omega_s, k_s^\perp) \hat{a}^\dagger(\omega_i, k_i^\perp) |0\rangle.\end{aligned}\quad (2.40)$$

This form of the output state will be the starting point of all considerations in the fourth chapter, where we calculate Schmidt modes of this state. In order to achieve this goal, we introduce the concept of Schmidt decomposition in the next chapter.

## Chapter 3

# Schmidt Decomposition

### 3.1 Quantum Entanglement

Quantum mechanics postulates that the state space  $\mathcal{H}$  of the composite system is the tensor product of state spaces  $\mathcal{H}_i$  of individual components

$$\mathcal{H} = \mathcal{H}_1 \otimes \mathcal{H}_2 \otimes \dots \otimes \mathcal{H}_n. \quad (3.1)$$

Another postulate states that the superposition of states is always a state<sup>1</sup>.

As a consequence of these postulates there exist some states of composite systems which can not be written in the form of a tensor product of states of individual components. We can illustrate this fact on simple case of two component system, where the subsystems are identical particles. Let  $\{|0\rangle, |1\rangle\}$  is the orthonormal basis of both subsystems. Then (neglecting the requirement for symmetry or antisymmetry of resulting vector)  $\{|0\rangle|0\rangle, |0\rangle|1\rangle, |1\rangle|0\rangle, |1\rangle|1\rangle\}$  is the orthonormal basis of whole system. But it is obvious that the vector

$$\frac{1}{\sqrt{2}}(|0\rangle|1\rangle + |1\rangle|0\rangle) = \frac{1}{\sqrt{2}} \begin{pmatrix} 0 \\ 1 \\ 1 \\ 0 \end{pmatrix} \quad (3.2)$$

can not be written as a product of states of individual components. To proof that statement, let us assume that the factorization exists, so we may write

$$\frac{1}{\sqrt{2}} \begin{pmatrix} 0 \\ 1 \\ 1 \\ 0 \end{pmatrix} = \begin{pmatrix} \alpha \\ \beta \end{pmatrix} \otimes \begin{pmatrix} \gamma \\ \delta \end{pmatrix} = \begin{pmatrix} \alpha\gamma \\ \alpha\delta \\ \beta\gamma \\ \beta\delta \end{pmatrix}, \quad (3.3)$$

---

<sup>1</sup>Generally this is not true because the realizable physical states may be limited by the so-called superselection rules. But this situation is of no interest to this work, therefore we assume that arbitrary superposition of physically realizable states is also realizable.

where the vectors are represented in the bases introduced above. However, this vector equation has no solution and therefore the discussed state is non-factorizable.

Entangled states play a crucial role in quantum computation and quantum information (for example the dense coding, Shor's factorization algorithm, Grover's search algorithm, selected quantum key distribution protocols, etc.) and are essential for quantum teleportation. Entanglement is the source of strong correlations in some degrees of freedom of entangled particles.

The above definition of entanglement is valid only for the pure ones. There exists generalization for mixed states but we do not introduce it because this work deals only with pure states. In the next section, we discuss how to quantify the amount of entanglement in quantum states.

### 3.2 Reduced States and von Neumann Entropy

As we have seen, for some states of the composite systems, we are not able to assign pure states of individual subsystems because the state is not separable. For this purpose, we introduce the idea of reduced density operator.

Let us have a two-component system  $AB$  with corresponding Hilbert space  $\mathcal{H} = \mathcal{H}_A \otimes \mathcal{H}_B$  where  $\left\{ \left| f_m^{(A)} \right\rangle \right\}_{m=1}^M$ ,  $\left\{ \left| g_n^{(B)} \right\rangle \right\}_{n=1}^N$  are the orthonormal bases of the subsystems. Let the system be in the pure state described by the vector  $|\Psi\rangle \in \mathcal{H}$ . Then, we may assign to the system the density operator

$$\hat{\rho} = |\Psi\rangle \langle \Psi|. \quad (3.4)$$

The state of the subsystem  $A$  is then given as the partial trace over the basis of the subsystem  $B$

$$\hat{\rho}_A = \text{Tr}_B \hat{\rho} = \sum_n \left\langle g_n^{(B)} \left| |\Psi\rangle \langle \Psi| \right| g_n^{(B)} \right\rangle. \quad (3.5)$$

We call  $\hat{\rho}_A$  reduced density operator of the subsystem  $A$ . Analogous definition is valid for the subsystem  $B$

$$\hat{\rho}_B = \text{Tr}_A \hat{\rho} = \sum_m \left\langle f_m^{(A)} \left| |\Psi\rangle \langle \Psi| \right| f_m^{(A)} \right\rangle. \quad (3.6)$$

For the state given by (3.2), we have

$$\hat{\rho}_A = \hat{\rho}_B = \frac{1}{2} (|0\rangle \langle 0| + |1\rangle \langle 1|). \quad (3.7)$$

We see that the subsystems are in the mixed states albeit the whole system is in the pure state.

In order to quantify the amount of entanglement, we introduce the concept of von Neumann entropy, being a straightforward generalization of Boltzmann

entropy in classical statistical mechanics [16]. It is defined for the state described by the density operator  $\hat{\rho}$  as

$$S(\hat{\rho}) = -\text{Tr}(\hat{\rho} \ln \hat{\rho}). \quad (3.8)$$

In the finite-dimensional case, it can be calculated easily using the formula

$$S(\hat{\rho}) = -\sum_n \lambda_n \ln \lambda_n, \quad (3.9)$$

where  $\lambda_n$  are the eigenvalues of  $\hat{\rho}$  and we set  $0 \ln 0 = 0$ . In the case of infinite dimension, we have to employ the functional calculus

$$\hat{\rho} \ln \hat{\rho} = \int \lambda \ln \lambda dE_\rho(\lambda), \quad (3.10)$$

where  $E_\rho(\lambda)$  is the projection-valued measure satisfying

$$\hat{\rho} = \int \lambda dE_\rho(\lambda). \quad (3.11)$$

The von Neumann entropy satisfies the so-called subadditive property [17], meaning that for bipartite state of system  $AB$  represented by density operator  $\hat{\rho}$ , it holds

$$S(\hat{\rho}) \leq S(\hat{\rho}_A) + S(\hat{\rho}_B), \quad (3.12)$$

where the equality holds if and only if the state is factorizable. This fact can lead us to define the index of correlation [16]

$$I_C = S(\hat{\rho}_A) + S(\hat{\rho}_B) - S(\hat{\rho}). \quad (3.13)$$

But more often we meet with the definition of so-called entropy of entanglement. For the given state  $|\Psi\rangle$ , we calculate the amount of entanglement as the von Neumann entropy of the reduced state  $S(\hat{\rho}_A)$ . We show in the following section that the definition is independent of the choice of the subsystem, i.e.  $S(\hat{\rho}_A) = S(\hat{\rho}_B)$ . The value of  $S(\hat{\rho}_A)$  for the separable state  $|\Psi\rangle = |f_m^{(A)}\rangle |g_n^{(B)}\rangle$  is zero because  $\hat{\rho}_A = |f_m^{(A)}\rangle \langle f_m^{(A)}|$  is one-dimensional projector on the subspace spanned by  $|f_m^{(A)}\rangle$ , and hence

$$S(\hat{\rho}_A) = -1 \ln 1 = 0. \quad (3.14)$$

On the other hand, to the maximum entangled state, it belongs the reduced density operator represented (in the finite-dimensional case) by diagonal matrix  $\rho_A = \text{diag}(\frac{1}{N}, \frac{1}{N}, \dots, \frac{1}{N})$ , where  $N$  is the order of the matrix. Then the von Neumann entropy is given as

$$S(\hat{\rho}_A) = -\sum_{n=1}^N \frac{1}{N} \ln \frac{1}{N} = \ln N. \quad (3.15)$$

There exist many other entanglement measures, defined for instance as a distance of the state from the set of separable states. Further details can be found in [18]. More detailed informations to reduced states (especially with respect to infinite-dimensional spaces) can be found in [19].

### 3.3 Schmidt Decomposition

In the following, we introduce the concept of Schmidt modes, Schmidt coefficients and Schmidt number (named after Baltic German mathematician Erhard Schmidt). As we shall see, Schmidt decomposition is very useful when manipulating with the entangled states.

Suppose that  $AB$  is a composite system consisting of subsystems  $A$  and  $B$ . Let  $|\Psi\rangle$  is the pure state of the system  $AB$  and let  $\left\{ \left| f_m^{(A)} \right\rangle \right\}_{m=1}^M, \left\{ \left| g_n^{(B)} \right\rangle \right\}_{n=1}^N$  are the orthonormal bases of the individual subsystems. Then we can write the state  $|\Psi\rangle$  in the form

$$|\Psi\rangle = \sum_{m,n} c_{m,n} \left| f_m^{(A)} \right\rangle \left| g_n^{(B)} \right\rangle. \quad (3.16)$$

It is possible to find two adjoint orthonormal bases  $\left\{ \left| \varphi_m^{(A)} \right\rangle \right\}, \left\{ \left| \chi_n^{(B)} \right\rangle \right\}$  unique for any given  $|\Psi\rangle$ , in which the double summation reduces to a single summation

$$|\Psi\rangle = \sum_m \sqrt{\lambda_m} \left| \varphi_m^{(A)} \right\rangle \left| \chi_m^{(B)} \right\rangle. \quad (3.17)$$

This representation of the state  $|\Psi\rangle$  is called the Schmidt decomposition and the non-negative numbers  $\sqrt{\lambda_m}$  are called Schmidt coefficients. The states  $\left\{ \left| \varphi_m^{(A)} \right\rangle \right\}$  and  $\left\{ \left| \chi_n^{(B)} \right\rangle \right\}$  are called adjoint Schmidt modes. Supposing the normalization of the state  $|\Psi\rangle$  to one, the Schmidt coefficients also satisfy the normalization condition  $\sum_m \lambda_m = 1$ .

The proof of this statement is based on the so-called singular value decomposition theorem<sup>2</sup>. We start with the state in the form (3.16) and we define the matrix  $C = (c_{i,j}) \in \mathbb{C}^{M,N}$  and assume  $N \geq M$ . Now we can apply the singular value decomposition algorithm on this matrix

$$C = U\Sigma V^\dagger, \quad (3.18)$$

---

<sup>2</sup>Let matrix  $A \in \mathbb{C}^{m,n}$  with  $n \geq m$  be given. Then there exists unitary matrices  $U \in \mathbb{C}^{n,n}$  and  $V \in \mathbb{C}^{m,m}$  such that

$$A = U\Sigma V^* \text{ with } \Sigma = \begin{pmatrix} \Sigma_r & 0_{r,m-r} \\ 0_{n-r,r} & 0_{n-r,m-r} \end{pmatrix} \in \mathbb{R}^{n,m},$$

where  $\Sigma_r = \text{diag}(\sigma_1, \sigma_2, \dots, \sigma_r)$  is the diagonal matrix,  $\sigma_1 \geq \sigma_2 \geq \dots \geq \sigma_r \geq 0$  and  $r = \text{rank}(A)$ . The proof of this statement can be found in [20].

where  $U = (u_{i,j}) \in \mathbb{C}^{N,N}$ ,  $V = (v_{i,j}) \in \mathbb{C}^{M,M}$  are unitary matrices and

$$\Sigma = \begin{pmatrix} \Sigma_r & 0_{r,m-r} \\ 0_{n-r,r} & 0_{n-r,m-r} \end{pmatrix} \in \mathbb{R}^{N,M} \quad (3.19)$$

is a diagonal matrix, where  $\Sigma_r = \text{diag}(\sqrt{\lambda_1}, \sqrt{\lambda_2}, \dots, \sqrt{\lambda_r})$ ,  $\sqrt{\lambda_1} \geq \sqrt{\lambda_2} \geq \dots \geq \sqrt{\lambda_r}$  and  $0_{m,n}$  stands for  $(m \times n)$  zero block. We can re-write (3.18) in the form

$$c_{m,n} = \sum_l \sqrt{\lambda_l} u_{m,l} v_{n,l}^*, \quad (3.20)$$

leading to

$$|\Psi\rangle = \sum_{l,m,n} \sqrt{\lambda_l} u_{m,l} v_{n,l}^* |f_m^{(A)}\rangle |g_n^{(B)}\rangle. \quad (3.21)$$

We define  $|\varphi_l^{(A)}\rangle = \sum_m u_{m,l} |f_m^{(A)}\rangle$  and  $|\chi_l^{(B)}\rangle = \sum_n v_{n,l}^* |g_n^{(B)}\rangle$ , allowing us to write

$$|\Psi\rangle = \sum_l \sqrt{\lambda_l} |\varphi_l^{(A)}\rangle |\chi_l^{(B)}\rangle, \quad (3.22)$$

which is the state in the Schmidt form (3.17).

So far, we have considered only finite-dimensional spaces. However the original work of Erhard Schmidt [21] was focused on infinite-dimensional spaces. So, we briefly outline the idea of Schmidt decomposition involving the infinite-dimensional spaces. We represent the state of the whole system in the form

$$\Psi(x, y) = \sum_{m,n} c_{m,n} f_m^{(A)}(x) g_n^{(B)}(y), \quad (3.23)$$

where  $\{f_m^{(A)}(x)\}_{m \in \mathbb{N}}$ ,  $\{g_n^{(B)}(y)\}_{n \in \mathbb{N}}$  are the bases of the subsystems and  $x, y$  are the continuous variables corresponding to the individual subsystems. We expect that the state can be written in the decomposed form

$$\Psi(x, y) = \sum_m \sqrt{\lambda_m} \varphi_m^{(A)}(x) \chi_m^{(B)}(y), \quad (3.24)$$

where  $\{\varphi_m^{(A)}(x)\}_{m \in \mathbb{N}}$  and  $\{\chi_n^{(B)}(y)\}_{n \in \mathbb{N}}$  are new orthonormal bases of the Schmidt modes. We assume the state to be normalized to one

$$\int dx \int dy |\Psi(x, y)|^2 = 1. \quad (3.25)$$

Then, the Schmidt modes can be found, solving the coupled integral equations. We need to multiply (3.24) by  $\varphi_n^{(A)*}(x)$  (or by  $\chi_n^{(B)*}(y)$  respectively) and integrate over  $x$  (over  $y$ ) to obtain

$$\int dx \Psi(x, y) \varphi_n^{(A)*}(x) = \sum_m \sqrt{\lambda_m} \chi_m^{(B)}(y) \int dx \varphi_m^{(A)}(x) \varphi_n^{(A)*}(x) = \sqrt{\lambda_n} \chi_n^{(B)}(y),$$

$$\int dy \Psi(x, y) \chi_n^{(B)*}(y) = \sum_m \sqrt{\lambda_m} \varphi_m^{(A)}(x) \int dy \chi_m^{(B)}(y) \chi_n^{(B)*}(y) = \sqrt{\lambda_n} \varphi_n^{(A)}(x), \quad (3.26)$$

where we have used the orthonormality of the Schmidt modes. So, we have seen that, according to the original work of Erhard Schmidt, the Schmidt modes can be found as the eigenfunctions of the coupled integral equations, kernels of which are given by the bipartite wave function.

Another definition of Schmidt modes works with the reduced density matrices. First of all, the density matrix of the whole system is constructed

$$\rho(x, y; x', y') = \Psi(x, y) \Psi^\dagger(x', y'). \quad (3.27)$$

Subsequently, the reduced density matrices are obtained by integration over one of two variables

$$\begin{aligned} \rho_A(x, x') &= \int dy \rho(x, y; x', y), \\ \rho_B(y, y') &= \int dx \rho(x, y; x, y'). \end{aligned} \quad (3.28)$$

The Schmidt modes are then defined as the eigenfunction of two integral equations with kernels given by the reduced density matrices

$$\begin{aligned} \int dx \rho_A(x, x') \varphi_n^{(A)}(x') &= \lambda_n \varphi_n(x), \\ \int dy \rho_B(y, y') \chi_n^{(B)}(y') &= \lambda_n \chi_n(x). \end{aligned} \quad (3.29)$$

The Schmidt decomposition of the reduced density matrices reads (with the help of (3.24))

$$\begin{aligned} \rho_A(x, x') &= \sum_n \lambda_n \varphi_n^{(A)}(x) \varphi_n^{(A)*}(x'), \\ \rho_B(y, y') &= \sum_n \lambda_n \chi_n^{(B)}(y) \chi_n^{(B)*}(y'). \end{aligned} \quad (3.30)$$

These definitions, both employing the integral equations, are almost equivalent. However, the definition via the reduced density matrix is invariant to addition of arbitrary phase factor  $e^{i\phi}$ ,  $\phi \in \mathbb{R}$  to any given Schmidt mode (the defining equation will be still fulfilled). In contrast, the first mentioned definition determines the Schmidt modes completely (including their phase). Further details can be found in [22].

### 3.4 Schmidt number

Now, when we have introduced the Schmidt modes, we can define another entanglement measure for the bipartite states – the Schmidt number. Having

the state in the form of Schmidt decomposition (3.17)

$$|\Psi\rangle = \sum_m \sqrt{\lambda_m} |\varphi_m^{(A)}\rangle |\chi_m^{(B)}\rangle, \quad (3.31)$$

it is very easy to calculate the quantity

$$K = \frac{1}{\sum_m \lambda_m^2}. \quad (3.32)$$

This number is called the Schmidt number and, as we have mentioned, it can be understood as another entanglement measure.

We compare both measures on the case of bipartite system  $AB$ , consisting of two-level particles. Let  $\{|\varphi_i^{(A)}\rangle\}_{i=1}^2$  and  $\{|\chi_j^{(B)}\rangle\}_{j=1}^2$  are the bases consisting of the adjoint Schmidt modes, so the state of the system can be written as

$$|\Psi\rangle = \sqrt{\lambda_1} |\varphi_1^{(A)}\rangle |\chi_1^{(B)}\rangle + \sqrt{\lambda_2} |\varphi_2^{(A)}\rangle |\chi_2^{(B)}\rangle. \quad (3.33)$$

It follows that the reduced density operators can be represented by matrices

$$\rho_A = \rho_B = \begin{pmatrix} \lambda_1 & 0 \\ 0 & \lambda_2 \end{pmatrix}. \quad (3.34)$$

Because the condition  $\lambda_1 + \lambda_2 = 1$  holds, we can parametrize the state setting  $\lambda_1 = \lambda$  and  $\lambda_2 = 1 - \lambda$ , where  $\lambda \in [0, 1]$ . The von Neumann entropy is then given by

$$S(\rho_A) = S(\rho_B) = -\lambda \ln \lambda - (1 - \lambda) \ln(1 - \lambda), \quad (3.35)$$

while the Schmidt number is

$$K = \frac{1}{\lambda^2 + (1 - \lambda)^2}. \quad (3.36)$$

The plot of both measure is on Figure 3.1 where we can see that they share the same intervals of increase and decrease, as would be expected.

As we said, we show that the von Neumann entropy of the reduced state is independent of the choice of the subsystem whose basis is used in the operation of the partial trace. From the existence of Schmidt decomposition, it immediately follows that the reduced density operators can be represented as  $\rho_A = \rho_B = \text{diag}(\lambda_1, \lambda_2, \dots, \lambda_N)$ , where  $\lambda_n$  are the squares of the Schmidt coefficients, and hence  $S(\rho_A) = S(\rho_B)$ .

Having introduced the Schmidt decomposition, we can move to the next chapter where we look for the Schmidt modes of parametric down-conversion in bulk crystals and in waveguide arrays.

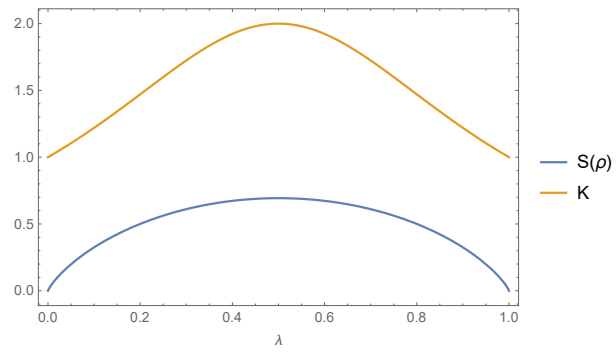


Figure 3.1: Comparison of entanglement measures (von Neumann entropy of the reduced state in blue and Schmidt number in orange) for the bipartite state given by 3.33 for  $\lambda_1 = \lambda$  and  $\lambda_2 = 1 - \lambda$ .

## Chapter 4

# Schmidt Modes of SPDC

### 4.1 Schmidt Modes of SPDC in Bulk Crystal

In this section, we will present how to obtain analytically the Schmidt modes of SPDC in bulk crystal, following [23, 24]. We start with the biphoton state given by (1.38), where the phase-matching function  $\Phi$  is given by (1.43)

$$\Phi(\mathbf{q}_s, \mathbf{q}_i) = \mathcal{N} \alpha(\mathbf{q}_s + \mathbf{q}_i) \operatorname{sinc} \left( \frac{|\mathbf{q}_s - \mathbf{q}_i|^2 L}{2k_p} \right),$$

where  $\mathcal{N}$  stands for the normalization and we expect  $\alpha(\mathbf{q}_s + \mathbf{q}_i)$  in the form of a Gaussian. Then we have

$$\Phi(\mathbf{q}_s, \mathbf{q}_i) = \mathcal{N} \exp \left[ -\frac{|\mathbf{q}_s + \mathbf{q}_i|^2}{\sigma^2} \right] \operatorname{sinc} \left( \frac{|\mathbf{q}_s - \mathbf{q}_i|^2 L}{2k_p} \right). \quad (4.1)$$

To obtain analytic solution, we replace the sinc function by its Gaussian approximation

$$\Phi(\mathbf{q}_s, \mathbf{q}_i) = \mathcal{N} \exp \left[ -\frac{|\mathbf{q}_s + \mathbf{q}_i|^2}{\sigma^2} \right] \exp \left[ -b^2 |\mathbf{q}_s - \mathbf{q}_i|^2 \right], \quad (4.2)$$

where

$$b = \frac{1}{2} \sqrt{\frac{L}{k_p}}. \quad (4.3)$$

Now, we have two options how to perform the decomposition. The first one is employing the Hermite polynomials (decomposition in Cartesian coordinates) and the second one uses the Laguerre polynomials (decomposition in polar coordinates).

#### 4.1.1 Decomposition in Cartesian Coordinates

First, we use the Hermite polynomials to find the decomposition. For this purpose we need to evaluate the following generating function (for details, see

[25])

$$\begin{aligned}
\sum_{n=0}^{+\infty} \frac{H_n(x)H_n(y)}{n!} t^n &= \\
&= \sum_{n=0}^{+\infty} \sum_{k=0}^{\lfloor n/2 \rfloor} \frac{(-1)^k n! (2x)^{n-2k}}{k!(n-2k)!} \frac{H_n(y)t^n}{n!} \\
&= \sum_{n=0}^{+\infty} \sum_{k=0}^{+\infty} \frac{(-1)^k (2x)^n H_{n+2k}(y) t^{n+2k}}{k!n!} \\
&= \sum_{k=0}^{+\infty} \left( \sum_{n=0}^{+\infty} \frac{H_{n+2k}(y)(2xt)^n}{n!} \right) \frac{(-1)^k t^{2k}}{k!} \\
&= \exp[4xyt - 4x^2t^2] \sum_{k=0}^{+\infty} \frac{(-1)^k H_{2k}(y - 2xt) t^{2k}}{k!} \\
&= \exp[4xyt - 4x^2t^2] \\
&\quad \times \sum_{k=0}^{+\infty} \sum_{l=0}^k \frac{(-1)^{k+l} 2^{2k} (\frac{1}{2})_k (2y - 4xt)^{2k-2l} t^{2k}}{l!(2k-2l)!} \\
&= \exp[4xyt - 4x^2t^2] \\
&\quad \times \sum_{k=0}^{+\infty} \sum_{l=0}^{+\infty} \frac{(-1)^k 2^{2k+2l} (\frac{1}{2})_{k+l} (2y - 4xt)^{2k} t^{2k+2l}}{l!(2k)!} \\
&= \exp[4xyt - 4x^2t^2] \\
&\quad \times \sum_{k=0}^{+\infty} \sum_{l=0}^{+\infty} \frac{(-1)^k 2^{2l} (\frac{1}{2})_{k+l} (2y - 4xt)^{2k} t^{2k+2l}}{l!k! (\frac{1}{2})_k} \\
&= \exp[4xyt - 4x^2t^2] \\
&\quad \times \sum_{k=0}^{+\infty} \left( \sum_{l=0}^{+\infty} \frac{(\frac{1}{2} + k)_l 2^{2l} t^{2l}}{l!} \right) \frac{(-1)^k (2y - 4xt)^{2k} t^{2k}}{k!} \\
&= \exp[4xyt - 4x^2t^2] \sum_{k=0}^{+\infty} \frac{(-1)^k (2y - 4xt)^{2k} t^{2k}}{k!(1-4t^2)^{1/2+k}} \\
&= (1-4t^2)^{-1/2} \exp \left[ \left( \frac{-4t^2}{1-4t^2} \right) \left( x^2 + y^2 - \frac{1}{t} xy \right) \right], \tag{4.4}
\end{aligned}$$

where  $H_n(x)$  is the  $n$ -th order Hermite polynomial. We introduce the so-called Hermite-Gaussian polynomials

$$h_n(\Gamma x) = \sqrt{\frac{\Gamma}{n!2^n\sqrt{\pi}}} e^{-\Gamma^2 x^2/2} H_n(\Gamma x), \tag{4.5}$$

where  $\Gamma$  is the scaling factor. Using (4.4), it is easy to write

$$\begin{aligned}
\sum_{n=0}^{+\infty} h_n(\Gamma x) h_n(\Gamma y) t^n &= \sum_{n=0}^{+\infty} \frac{\sqrt{\Gamma} e^{-\Gamma^2 x^2/2} H_n(\Gamma x)}{(n! 2^n \sqrt{\pi})^{1/2}} \frac{\sqrt{\Gamma} e^{-\Gamma^2 y^2/2} H_n(\Gamma y)}{(n! 2^n \sqrt{\pi})^{1/2}} t^n \\
&= \frac{\Gamma e^{-\Gamma^2(x^2+y^2)/2}}{\sqrt{\pi}} \sum_{n=0}^{+\infty} \frac{H_n(\Gamma x) H_n(\Gamma y)}{n!} \left(\frac{t}{2}\right)^n \\
&= \frac{\Gamma e^{-\Gamma^2(x^2+y^2)/2}}{\sqrt{\pi}} (1-t^2)^{-1/2} \\
&\quad \times \exp \left[ \left( -\frac{t^2}{1-t^2} \right) \left( \Gamma^2 x^2 + \Gamma^2 y^2 - \frac{2}{t} \Gamma^2 xy \right) \right] \\
&= \frac{\Gamma}{\sqrt{\pi}} (1-t^2)^{-1/2} \\
&\quad \times \exp \left[ \left( -\frac{\Gamma^2}{2} \frac{1+t^2}{1-t^2} \right) \left( x^2 + y^2 - 2 \left( \frac{2t}{1+t^2} \right) xy \right) \right].
\end{aligned} \tag{4.6}$$

We re-write equation (4.2) as

$$\begin{aligned}
\Phi(\mathbf{q}_s, \mathbf{q}_i) &= \mathcal{N} \exp \left[ - \left( b^2 + \frac{1}{\sigma^2} \right) (q_{s1}^2 + q_{i1}^2) + 2 \left( b^2 - \frac{1}{\sigma^2} \right) q_{s1} q_{i1} \right] \\
&\quad \times \exp \left[ - \left( b^2 + \frac{1}{\sigma^2} \right) (q_{s2}^2 + q_{i2}^2) + 2 \left( b^2 - \frac{1}{\sigma^2} \right) q_{s2} q_{i2} \right],
\end{aligned} \tag{4.7}$$

where  $\mathbf{q}_s = (q_{s1}, q_{s2})$  and  $\mathbf{q}_i = (q_{i1}, q_{i2})$ . Setting

$$\begin{aligned}
G &= b^2 + \frac{1}{\sigma^2}, \\
\eta &= \frac{b^2 \sigma^2 - 1}{b^2 \sigma^2 + 1},
\end{aligned} \tag{4.8}$$

we may write

$$\Phi(\mathbf{q}_s, \mathbf{q}_i) = \mathcal{N} \exp [-G (q_{s1}^2 + q_{i1}^2 - 2\eta q_{s1} q_{i1})] \exp [-G (q_{s2}^2 + q_{i2}^2 - 2\eta q_{s2} q_{i2})]. \tag{4.9}$$

Comparing the last expression with (4.6), we have to set

$$\begin{aligned}
G &= \frac{\Gamma^2}{2} \frac{1+t^2}{1-t^2}, \\
\eta &= \frac{2t}{1+t^2}.
\end{aligned} \tag{4.10}$$

These relation can be inverted, leading to

$$t = \frac{|G\eta|}{|G + \Gamma^2/2|} = \frac{|b\sigma - 1|}{|b\sigma + 1|},$$

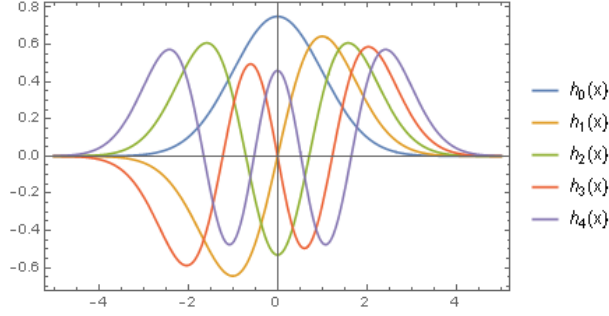


Figure 4.1: Plot of the first five Hermite-Gaussian polynomials, given by (4.5), for value  $\Gamma = 1$ .

$$\Gamma = \sqrt{\frac{4b}{\sigma}}. \quad (4.11)$$

Finally, we may express the state in the form of the Schmidt decomposition

$$\Phi(\mathbf{q}_s, \mathbf{q}_i) = \mathcal{N}(1 - t^2) \sum_{m,n} t^{m+n} h_m(\Gamma q_{s1}) h_m(\Gamma q_{i1}) h_n(\Gamma q_{s2}) h_n(\Gamma q_{i2}). \quad (4.12)$$

Plots of first few Hermite-Gaussian polynomials are on Figure 4.1.

#### 4.1.2 Decomposition in Polar Coordinates

We transform the state (4.2) from the Cartesian coordinates to the polar coordinates  $\mathbf{q} = (\rho \cos(\varphi), \rho \sin(\varphi))$  leading to

$$\begin{aligned} \Phi &= \mathcal{N} \exp \left[ -\frac{|\mathbf{q}'_s + \mathbf{q}'_i|^2}{\sigma^2} \right] \exp \left[ -b^2 |\mathbf{q}'_s - \mathbf{q}'_i|^2 \right] \\ &= \mathcal{N} \exp \left[ -\frac{\rho_s^2 + \rho_i^2 + 2\rho_s \rho_i (\cos \varphi_s \cos \varphi_i + \sin \varphi_s \sin \varphi_i)}{\sigma^2} \right] \\ &\quad \times \exp \left[ -b^2 (\rho_s^2 + \rho_i^2 - 2\rho_s \rho_i (\cos \varphi_s \cos \varphi_i + \sin \varphi_s \sin \varphi_i)) \right] \\ &= \mathcal{N} \exp \left[ -\frac{\rho_s^2 + \rho_i^2 + 2\rho_s \rho_i \cos(\varphi_s - \varphi_i)}{\sigma^2} \right] \\ &\quad \times \exp \left[ -b^2 (\rho_s^2 + \rho_i^2 - 2\rho_s \rho_i \cos(\varphi_s - \varphi_i)) \right] \\ &= \mathcal{N} \exp \left[ -(\rho_s^2 + \rho_i^2) \left( b^2 + \frac{1}{\sigma^2} \right) \right] \exp \left[ 2\rho_s \rho_i \cos(\varphi_s - \varphi_i) \left( b^2 - \frac{1}{\sigma^2} \right) \right]. \end{aligned} \quad (4.13)$$

We utilize that the function is dependent just on the difference of the angular variables  $\varphi_s - \varphi_i$  and we perform Fourier transform

$$\Phi = \sum_{j=-\infty}^{+\infty} \sqrt{P_j} F_j(\rho_s, \rho_i) e^{ij(\varphi_s - \varphi_i)}, \quad (4.14)$$

where the Fourier components are given by

$$\begin{aligned}\sqrt{P_j}F_j(\rho_s, \rho_i) &= \frac{1}{2\pi}\mathcal{N} \exp\left[-(\rho_s^2 + \rho_i^2)\left(b^2 + \frac{1}{\sigma^2}\right)\right] \\ &\times \int_{-\pi}^{\pi} d(\varphi_s - \varphi_i) \exp\left[2\rho_s\rho_i\left(b^2 - \frac{1}{\sigma^2}\right)\cos(\varphi_s - \varphi_i)\right] \\ &\times e^{-ij(\varphi_s - \varphi_i)}.\end{aligned}\quad (4.15)$$

According to [26] the  $j$ -th order modified Bessel function of the first kind can be expressed for any integer  $j$  in the form

$$I_j(z) = \frac{1}{\pi} \int_0^\pi e^{z \cos \varphi} \cos j\varphi d\varphi. \quad (4.16)$$

It follows that

$$\sqrt{P_j}F_j(\rho_s, \rho_i) = \mathcal{N} \exp\left[-(\rho_s^2 + \rho_i^2)\left(b^2 + \frac{1}{\sigma^2}\right)\right] I_{|j|}\left(2\rho_s\rho_i\left(b^2 - \frac{1}{\sigma^2}\right)\right). \quad (4.17)$$

Now, we use the following identity

$$\sum_{p=0}^{+\infty} \mu^{2p} r_p^{(j)}(x) r_p^{(j)}(y) = \frac{|\mu|^{-|j|}}{1 - \mu^2} e^{-\frac{x^2+y^2}{2} \frac{1+\mu^2}{1-\mu^2}} I_{|j|}\left(2xy \frac{|\mu|}{\mu^2 - 1}\right), \quad (4.18)$$

where the Laguerre-Gaussian polynomials are given by

$$r_p^{(j)}(x) = \sqrt{\frac{2p!}{(p+|j|)!}} e^{-\frac{x^2}{2}} x^{|j|} L_p^{(|j|)}(x^2) \quad (4.19)$$

and  $L_p^{(j)}$  are the generalized Laguerre polynomial. The proof of (4.18) can be found in [27]. We rescale the Laguerre-Gaussian polynomials  $r_p^{(j)}(\rho) \rightarrow r_p^{(j)}(\Gamma\rho)$  and comparing the equations (4.17) and (4.18) leads us to the requirements

$$\begin{aligned}\Gamma^2 \frac{|\mu|}{\mu^2 - 1} &= b^2 - \frac{1}{\sigma^2}, \\ \frac{\Gamma^2}{2} \frac{1 + \mu^2}{1 - \mu^2} &= b^2 + \frac{1}{\sigma^2}.\end{aligned}\quad (4.20)$$

These equations are satisfied for

$$\begin{aligned}\mu^2 &= \left(\frac{1 - b\sigma}{1 + b\sigma}\right)^2, \\ \Gamma &= \sqrt{\frac{4b}{\sigma}}.\end{aligned}\quad (4.21)$$

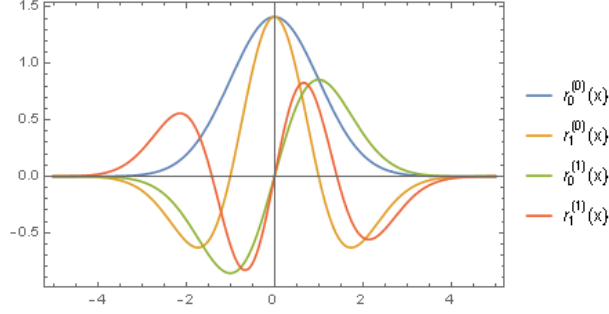


Figure 4.2: First few Laguerre-Gaussian polynomials given by (4.19). Again, we have set  $\Gamma = 1$ .

Finally, we may write

$$\Phi = \mathcal{N}(1 - \mu^2) \sum_{j=-\infty}^{+\infty} \sum_{p=0}^{+\infty} \mu^{2p+|j|} r_p^{(j)}(\Gamma\rho_s) e^{ij\varphi_s} r_p^{(j)}(\Gamma\rho_i) e^{-ij\varphi_i}. \quad (4.22)$$

On Figure 4.2, we plot first few Laguerre-Gaussian polynomials. The question of equivalence of the calculated Schmidt bases is discussed in [24].

## 4.2 Schmidt Modes of SPDC in Waveguide Array

In this section, we derive the Schmidt modes of parametric down-conversion in an waveguide array. We start with the biphoton SPDC given by (2.40) and we add two additional factors  $F(\omega_s)$ ,  $F(\omega_i)$  representing the spectral filters placed in front of the detectors

$$f(\omega_s, \omega_i, k_s^\perp, k_i^\perp) = \mathcal{N} \alpha(\omega_s + \omega_i) F(\omega_s) F(\omega_i) \sum_n A_n e^{-i(k_s^\perp + k_i^\perp)n} \times e^{-i\Delta\beta(\omega_s, \omega_i, k_s^\perp, k_i^\perp) \frac{L}{2}} \text{sinc} \left( \Delta\beta(\omega_s, \omega_i, k_s^\perp, k_i^\perp) \frac{L}{2} \right). \quad (4.23)$$

We expect the spectral shape of the pump and the filtering functions as Gaussians

$$\alpha(\omega_s + \omega_i) F(\omega_s) F(\omega_i) = \exp \left[ -\frac{(\omega_s + \omega_i - \omega_0)^2}{2\sigma_p^2} \right] \exp \left[ -\frac{(\omega_s - \omega_1)^2}{2\sigma_s^2} \right] \times \exp \left[ -\frac{(\omega_i - \omega_2)^2}{2\sigma_i^2} \right], \quad (4.24)$$

where  $\omega_j$  is the central frequency and  $\sigma_j$  is the standard deviation of the distribution. We expect that the condition  $\omega_0 \approx \omega_1 + \omega_2$  holds (representing the energy conservation). Our state is then given by

$$f(\tilde{\omega}_s, \tilde{\omega}_i, k_s^\perp, k_i^\perp) \approx \mathcal{N} \exp \left[ -\frac{\tilde{\omega}_s^2 + \tilde{\omega}_i^2}{2\sigma^2} \right] \sum_n A_n e^{-i(k_s^\perp + k_i^\perp)n}$$

$$\times \int_0^1 dt \exp \left[ -i \Delta \beta(\tilde{\omega}_s, \tilde{\omega}_i, k_s^\perp, k_i^\perp) L t \right], \quad (4.25)$$

where we have employed the following identity<sup>1</sup>

$$e^{-i\frac{x}{2}} \operatorname{sinc} \left( \frac{x}{2} \right) = \int_0^1 dt e^{-ixt}, \quad (4.26)$$

and we have set  $\tilde{\omega}_s = \omega_s - \omega_1$  and  $\tilde{\omega}_i = \omega_i - \omega_2$ . We approximate the frequency-dependent part of the phase-mismatch

$$\Delta \beta^{(0)}(\omega_s, \omega_i) = \beta_p^{(0)}(\omega_s + \omega_i) - \beta^{(0)}(\omega_s) - \beta^{(0)}(\omega_i) \quad (4.27)$$

by its Taylor expansion up to the first order and we replace the coupling coefficients  $C(\omega)$  by constants  $C_s = C(\omega_1)L$ ,  $C_i = C(\omega_2)L$ , leading to

$$\Delta \beta(\tilde{\omega}_s, \tilde{\omega}_i, k_s^\perp, k_i^\perp) L \approx a + b_s \tilde{\omega}_s + b_i \tilde{\omega}_i - 2C_s \cos(k_s^\perp) - 2C_i \cos(k_i^\perp), \quad (4.28)$$

where

$$\begin{aligned} a &= \Delta \beta^{(0)}(\omega_1, \omega_2) L, \\ b_j &= \left. \frac{\partial (\Delta \beta^{(0)}(\omega_s, \omega_i))}{\partial \omega_j} \right|_{\omega_s=\omega_1, \omega_i=\omega_2} L. \end{aligned} \quad (4.29)$$

Note, that we have incorporated the waveguide length  $L$  into the constants for simplicity. We may rewrite (4.25) as

$$\begin{aligned} f(\tilde{\omega}_s, \tilde{\omega}_i, k_s^\perp, k_i^\perp) &\approx \mathcal{N} \sum_n A_n e^{-i(k_s^\perp + k_i^\perp)n} \\ &\times \int_0^1 dt e^{-iat} \exp \left[ - \left( \frac{1}{2\sigma_p^2} + \frac{1}{2\sigma_s^2} \right) \tilde{\omega}_s^2 - ib_s t \tilde{\omega}_s \right] \\ &\times \exp \left[ - \frac{1}{\sigma_p^2} \tilde{\omega}_s \tilde{\omega}_i \right] \exp \left[ - \left( \frac{1}{2\sigma_p^2} + \frac{1}{2\sigma_i^2} \right) \tilde{\omega}_i^2 - ib_i t \tilde{\omega}_i \right] \\ &\times \exp \left[ i \left( 2C_s \cos(k_s^\perp) + 2C_i \cos(k_i^\perp) \right) t \right]. \end{aligned} \quad (4.30)$$

Now, we calculate the Fourier coefficients with respect to the orthonormal bases  $\left\{ \sqrt{\frac{\Gamma}{2^n n! \sqrt{\pi}}} e^{-\Gamma^2 \omega^2 / 2} H_n(\Gamma \omega) \right\}_{n \in \mathbf{N}}$  and  $\left\{ \frac{1}{\sqrt{2\pi}} e^{ik^\perp} \right\}_{l \in \mathbf{Z}}$ . The first one contains orthonormal Hermite-Gaussian polynomials which are used for the decomposition in the frequency coordinates  $\tilde{\omega}_s$  and  $\tilde{\omega}_i$ . The parameter  $\Gamma$  is the scaling factor and we specify it later. The second basis contains trigonometric polynomials and it will be used for the decomposition in the spatial coordinates  $k_s^\perp$  and  $k_i^\perp$ . Thus, let us set

$$c_{j,k,l,m} = \int_{-\infty}^{+\infty} d\tilde{\omega}_s \int_{-\infty}^{+\infty} d\tilde{\omega}_i \int_{-\pi}^{\pi} dk_s^\perp \int_{-\pi}^{\pi} dk_i^\perp \sqrt{\frac{\Gamma_s}{2^k k! \sqrt{\pi}}} e^{-\Gamma_s^2 \tilde{\omega}_s^2 / 2} H_j(\Gamma_s \tilde{\omega}_s)$$

<sup>1</sup>In fact, we are returning to (2.34) when the integration in the  $z$  coordinate has been performed.

$$\begin{aligned}
& \times \sqrt{\frac{\Gamma_i}{2^l l! \sqrt{\pi}}} e^{-\Gamma_i^2 \tilde{\omega}_i^2 / 2} H_k(\Gamma_i \tilde{\omega}_i) \frac{e^{-i l k_s^\perp}}{\sqrt{2\pi}} \frac{e^{-i m k_i^\perp}}{\sqrt{2\pi}} f(\tilde{\omega}_s, \tilde{\omega}_i, k_s^\perp, k_i^\perp) \\
& = \frac{\mathcal{N}}{2\pi} \sqrt{\frac{\Gamma_s \Gamma_i}{2^{j+k} j! k! \pi}} \sum_n A_n \int_0^1 dt e^{-iat} \\
& \quad \times \int_{-\pi}^{\pi} dk_s^\perp e^{-i(l+n)k_s^\perp} \exp\left[i2C_s t \cos(k_s^\perp)\right] \\
& \quad \times \int_{-\pi}^{\pi} dk_i^\perp e^{-i(m+n)k_i^\perp} \exp\left[i2C_i t \cos(k_i^\perp)\right] \\
& \quad \times \int_{-\infty}^{+\infty} d\tilde{\omega}_i \exp\left[-\left(\frac{1}{2\sigma_p^2} + \frac{1}{2\sigma_i^2} + \frac{\Gamma_i^2}{2}\right) \tilde{\omega}_i^2 - ib_i t \tilde{\omega}_i\right] H_k(\Gamma_i \tilde{\omega}_i) \\
& \quad \times \int_{-\infty}^{+\infty} d\tilde{\omega}_s \exp\left[-\left(\frac{1}{2\sigma_p^2} + \frac{1}{2\sigma_s^2} + \frac{\Gamma_s^2}{2}\right) \tilde{\omega}_s^2 - \left(\frac{1}{\sigma_p^2} \tilde{\omega}_i + ib_s t\right) \tilde{\omega}_s\right] \\
& \quad \times H_j(\Gamma_s \tilde{\omega}_s). \tag{4.31}
\end{aligned}$$

Once more, we employ (4.16) and we set the scaling factor  $\Gamma_s$  such, that

$$\frac{1}{2\sigma_p^2} + \frac{1}{2\sigma_s^2} + \frac{\Gamma_s^2}{2} = \Gamma_s^2 \tag{4.32}$$

holds, i.e.  $\Gamma_s = \sqrt{1/\sigma_p^2 + 1/\sigma_s^2}$ . Under this condition, we may use the so-called Rodrigues formula [25]

$$e^{-x^2} H_n(x) = (-1)^n \frac{d^n}{dx^n} \left( e^{-x^2} \right) \tag{4.33}$$

and we may write

$$\begin{aligned}
c_{j,k,l,m} & = 2\pi \mathcal{N} \sqrt{\frac{\Gamma_s \Gamma_i}{2^{j+k} j! k! \pi}} \sum_n A_n \int_0^1 dt e^{-iat} I_{|l+n|}(i2C_s t) I_{|m+n|}(i2C_i t) \\
& \quad \times \int_{-\infty}^{+\infty} d\tilde{\omega}_i \exp\left[-\left(\frac{1}{2\sigma_p^2} + \frac{1}{2\sigma_i^2} + \frac{\Gamma_i^2}{2}\right) \tilde{\omega}_i^2 - ib_i t \tilde{\omega}_i\right] H_k(\Gamma_i \tilde{\omega}_i) \\
& \quad \times \int_{-\infty}^{+\infty} d\tilde{\omega}_s \exp\left[-\left(\frac{1}{\sigma_p^2} \tilde{\omega}_i + ib_s t\right) \tilde{\omega}_s\right] \frac{(-1)^j}{\Gamma_s^j} \frac{d^j}{d\tilde{\omega}_s^j} \left( e^{-\Gamma_s^2 \tilde{\omega}_s^2} \right). \tag{4.34}
\end{aligned}$$

We perform  $j$ -times integration by parts in the  $\tilde{\omega}_s$  coordinate

$$\begin{aligned}
c_{j,k,l,m} & = \frac{(-1)^j 2\pi \mathcal{N}}{\Gamma_s^j} \sqrt{\frac{\Gamma_s \Gamma_i}{2^{j+k} j! k! \pi}} \sum_n A_n \int_0^1 dt e^{-iat} I_{|l+n|}(i2C_s t) I_{|m+n|}(i2C_i t) \\
& \quad \times \int_{-\infty}^{+\infty} d\tilde{\omega}_i \exp\left[-\left(\frac{1}{2\sigma_p^2} + \frac{1}{2\sigma_i^2} + \frac{\Gamma_i^2}{2}\right) \tilde{\omega}_i^2 - ib_i t \tilde{\omega}_i\right] H_k(\Gamma_i \tilde{\omega}_i)
\end{aligned}$$

$$\begin{aligned}
& \times \left( \frac{1}{\sigma_p^2} \tilde{\omega}_i + ib_s t \right)^j \int_{-\infty}^{+\infty} d\tilde{\omega}_s \exp \left[ - \left( \frac{1}{\sigma_p^2} \tilde{\omega}_i + ib_s t \right) \tilde{\omega}_s \right] e^{-\Gamma_s^2 \tilde{\omega}_s^2} \\
& = \frac{(-1)^j 2\pi \mathcal{N}}{\Gamma_s^j} \sqrt{\frac{\Gamma_s \Gamma_i}{2^{j+k} j! k! \pi}} \sum_n A_n \int_0^1 dt e^{-iat} I_{|l+n|}(i2C_s t) I_{|m+n|}(i2C_i t) \\
& \quad \times \int_{-\infty}^{+\infty} d\tilde{\omega}_i \exp \left[ - \left( \frac{1}{2\sigma_p^2} + \frac{1}{2\sigma_i^2} + \frac{\Gamma_i^2}{2} \right) \tilde{\omega}_i^2 - ib_i t \tilde{\omega}_i \right] H_k(\Gamma_i \tilde{\omega}_i) \\
& \quad \times \left( \frac{1}{\sigma_p^2} \tilde{\omega}_i + ib_s t \right)^j \sqrt{\frac{\pi}{\Gamma_s^2}} \exp \left[ \frac{1}{4\Gamma_s^2} \left( \frac{1}{\sigma_p^2} \tilde{\omega}_i + ib_s t \right)^2 \right], \tag{4.35}
\end{aligned}$$

allowing us to easily evaluate the Gaussian integral.

We set also the scaling factor  $\Gamma_i$ , so we may use the Rodrigues formula again. We rearrange the arguments of the exponential functions

$$\begin{aligned}
c_{j,k,l,m} & = \frac{(-1)^j 2\pi \mathcal{N}}{\Gamma_s^j} \sqrt{\frac{\Gamma_i}{2^{j+k} j! k! \Gamma_s}} \sum_n A_n \int_0^1 dt e^{-iat - b_s^2 t^2 / 4\Gamma_s^2} \\
& \quad \times I_{|l+n|}(i2C_s t) I_{|m+n|}(i2C_i t) \\
& \quad \times \int_{-\infty}^{+\infty} d\tilde{\omega}_i \exp \left[ - \left( \frac{1}{2\sigma_p^2} + \frac{1}{2\sigma_i^2} - \frac{1}{4\Gamma_s^2 \sigma_p^4} + \frac{\Gamma_i^2}{2} \right) \tilde{\omega}_i^2 \right] H_k(\Gamma_i \tilde{\omega}_i) \\
& \quad \times \left( \frac{1}{\sigma_p^2} \tilde{\omega}_i + ib_s t \right)^j \exp \left[ i \left( \frac{b_s}{2\Gamma_s^2 \sigma_p^2} - b_i \right) t \tilde{\omega}_i \right], \tag{4.36}
\end{aligned}$$

leading to requirement

$$\frac{1}{2\sigma_p^2} + \frac{1}{2\sigma_i^2} - \frac{1}{4\Gamma_s^2 \sigma_p^4} + \frac{\Gamma_i^2}{2} = \Gamma_i^2. \tag{4.37}$$

Now, we can apply the Rodrigues formula and after the  $k$ -times integration by parts we have

$$\begin{aligned}
c_{j,k,l,m} & = \frac{(-1)^j 2\pi \mathcal{N}}{\Gamma_s^j \Gamma_i^k} \sqrt{\frac{\Gamma_i}{2^{j+k} j! k! \Gamma_s}} \sum_n A_n \int_0^1 dt e^{-iat - b_s^2 t^2 / 4\Gamma_s^2} \\
& \quad \times I_{|l+n|}(i2C_s t) I_{|m+n|}(i2C_i t) \\
& \quad \times \int_{-\infty}^{+\infty} d\tilde{\omega}_i \frac{d^k}{d\tilde{\omega}_i^k} \left( \left( \frac{1}{\sigma_p^2} \tilde{\omega}_i + ib_s t \right)^j \exp \left[ i \left( \frac{b_s}{2\Gamma_s^2 \sigma_p^2} - b_i \right) t \tilde{\omega}_i \right] \right) e^{-\Gamma_i^2 \tilde{\omega}_i^2}. \tag{4.38}
\end{aligned}$$

Using this final formula, the Fourier coefficients  $c_{j,k,l,m}$  can be easily calculated numerically. We calculate them for the finite set of indices and then use the singular value decomposition algorithm to find the Schmidt modes and Schmidt numbers. To perform the decomposition we define the matrix  $D$  with the elements

$$D_{jk} = c_{[j/(2M+1)], [k/(2M+1)], j - [j/(2M+1)](2M+1) - M, k - [k/(2M+1)](2M+1) - M}, \tag{4.39}$$

where  $\lfloor j \rfloor$  is the integer part of the number  $j$  and  $M$  is related to the cut-off in the momentum domain – we calculate the coefficients with respect to the set  $\left\{ \frac{1}{\sqrt{2\pi}} e^{ik^\perp} \right\}_{l=-M}^M$ . The indices  $j, k$  satisfy  $j, k \in \{0, 1, \dots, (2M+1)N-1\}$ , where  $N$  is related to the cut-off in the frequency domain – we are taking into consideration only Hermite-Gaussian polynomials from the finite set  $\left\{ \sqrt{\frac{\Gamma}{2^n n! \sqrt{\pi}}} e^{-\Gamma^2 \omega^2 / 2} H_n(\Gamma \omega) \right\}_{n=0}^{N-1}$ . Thus the matrix  $D$  has the following form

$$D = \begin{pmatrix} c_{0,0,-M,-M} & \cdots & c_{0,0,-M,M} & \cdots & c_{0,N-1,-M,M} \\ \vdots & \ddots & \vdots & & \vdots \\ c_{0,0,M,-M} & \cdots & c_{0,0,M,M} & & \vdots \\ \vdots & & & \ddots & \\ c_{N-1,0,M,-M} & & \cdots & & c_{N-1,N-1,M,M} \end{pmatrix}. \quad (4.40)$$

Then we find the matrices  $U, \Sigma, V$  such that

$$D = (d_{l,m}) = U \Sigma V^\dagger, \quad (4.41)$$

where  $U = (u_{i,j})$ ,  $V = (v_{i,j})$  are unitary matrices and  $\Sigma = \text{diag}(\sqrt{\lambda_j})$  is the diagonal matrix. The Schmidt modes are given by

$$\begin{aligned} g_j(\tilde{\omega}_s, k_s^\perp) &= \sum_{l=0}^{(2M+1)N-1} u_{l,j} G_l(\tilde{\omega}_s k_s^\perp), \\ h_j(\tilde{\omega}_i, k_i^\perp) &= \sum_{m=-N}^{(2M+1)N-1} v_{m,j}^* H_m(\tilde{\omega}_i, k_i^\perp). \end{aligned} \quad (4.42)$$

where we have set

$$\begin{aligned} G_j(\tilde{\omega}_s, k_s^\perp) &= \sqrt{\frac{\Gamma_s}{2^{\lfloor j/(2M+1) \rfloor + 1} (\lfloor j/(2M+1) \rfloor)! \pi}} e^{-\Gamma_s^2 \tilde{\omega}_s^2 / 2} H_{\lfloor j/(2M+1) \rfloor}(\Gamma_s \tilde{\omega}_s) \\ &\quad \times \exp \left[ i(j - \lfloor j/(2M+1) \rfloor)(2M+1) - M \right] k_s^\perp, \\ H_j(\tilde{\omega}_i, k_i^\perp) &= \sqrt{\frac{\Gamma_i}{2^{\lfloor j/(2M+1) \rfloor + 1} (\lfloor j/(2M+1) \rfloor)! \pi}} e^{-\Gamma_i^2 \tilde{\omega}_i^2 / 2} H_{\lfloor j/(2M+1) \rfloor}(\Gamma_i \tilde{\omega}_i) \\ &\quad \times \exp \left[ i(j - \lfloor j/(2M+1) \rfloor)(2M+1) - M \right] k_i^\perp. \end{aligned} \quad (4.43)$$

The decomposition then reads

$$f(\tilde{\omega}_s, \tilde{\omega}_i, k_s^\perp, k_i^\perp) \approx \sum_{j=0}^{(2M+1)N-1} \sqrt{\lambda_j} g_j(k_s^\perp) h_j(k_i^\perp). \quad (4.44)$$

The question of the effect of the cut-off was discussed in [28], identifying two sources of error. The first one is the truncation error. It decreases with the

growing  $M$  and  $N$  (the Fourier coefficients  $c_{j,k,l,m}$  tends to zero for  $j, k, l, m \rightarrow +\infty$ ) and it is also affected by the particular choice of the orthonormal bases (this choice determines the speed of convergence). The second source of error is the numerical error in calculating the coefficients  $c_{j,k,l,m}$  and the error when performing the singular value decomposition.

The Schmidt modes obtained by the method described above are presented in the following chapter.

## Chapter 5

# Numerical Results

The Schmidt modes and the Schmidt numbers were computed by the Mathematica software [29] for various input parameters, altering the wavelengths of generated photons and the illumination pattern. First, we introduce the parameters employed in our model (experimentally motivated and originally introduced in [14]), then we present three model cases.

### 5.1 Simulation Parameters

For the calculation of the Schmidt modes we have used parameters introduced in [14]. We expect the central wavelength of the pump at  $\lambda_p = 775.0$  nm and the bandwidth 0.8 nm, while the bandwidth of the detectors is expected to be 0.1 nm.

The spectral phase-mismatch is given by (4.27). We expect the quasi-phase-matching (1.21)

$$\Delta\beta^{(0)}(\omega_s, \omega_i) = \beta_p^{(0)}(\omega_s + \omega_i) - \beta^{(0)}(\omega_s) - \beta^{(0)}(\omega_i) - \frac{2\pi}{\Lambda},$$

where the poling period  $\Lambda$  is chosen such, that the perfect phase-matching is obtained for degenerate photon pairs at  $\lambda_s = \lambda_i = 1550$  nm. We expect the pump photons having the extraordinary polarization and the signal and idler photons having the ordinary polarization.

For calculating the propagation constants  $\beta^{(0)}(\omega) = \omega n(\omega)/c$ , we have used the wavelength- and temperature-dependent Sellmeier equations [30], describing the refractive index

$$n_i^2 = A_1 + \frac{A_2 + B_1 F}{\lambda^2 - (A_3 + B_2 F)^2} + B_3 F - A_4 \lambda^2, \quad (5.1)$$

where  $\lambda$  is the wavelength in micrometers. The temperature dependency is given by

$$F(T) = (T - T_0)(T + T_0 + 546),$$

	$n_o$	$n_e$
$A_1$	4.9048	4.5820
$A_2$	0.11775	0.09921
$A_3$	0.21802	0.21090
$A_4$	0.027153	0.021940
$B_1$	$2.2314 \times 10^{-8}$	$5.2716 \times 10^{-8}$
$B_2$	$-2.9671 \times 10^{-8}$	$-4.9143 \times 10^{-8}$
$B_3$	$2.1429 \times 10^{-8}$	$2.2971 \times 10^{-7}$

Table 5.1: The parameters from Sellmeier equation (5.1) for ordinary ( $n_o$ ) and extraordinary ( $n_e$ ) refractive indices. Taken from [30].

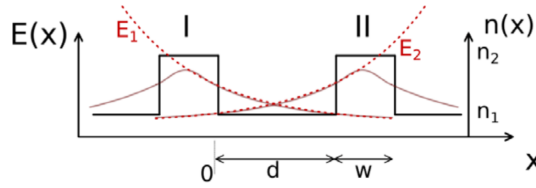


Figure 5.1: Form of electric fields for a rectangular refractive index profile. Taken from [14].

where  $T$  is the temperature in degrees Celsius and  $T_0 = 24.5^\circ\text{C}$ . For all simulations, we use the temperature value  $T = 185.0^\circ\text{C}$ . The values of the coefficients  $A$  are given in table 5.1.

To calculate the frequency dependent coupling constants, we have adopted the approach introduced in [14]. As we have derived in the second chapter, the coupling coefficient is given by (2.19) as the overlap integral from the mode of one of waveguides with the mode in the neighbouring waveguide. We can re-express the coupling in the terms of wavelength as

$$C(\lambda) \approx C_0 \frac{2\pi}{\lambda} \int \Delta n_k^2(x) \mathcal{E}_2(x) \cdot \mathcal{E}_1^*(x) dx. \quad (5.2)$$

We assume a simple model for the waveguide modes (see Figure 5.1), considering only the exponential part of the evanescent field

$$\begin{aligned} \mathcal{E}_1(x) &= \mathcal{E}_{10} e^{-\gamma x}, \\ \mathcal{E}_2(x) &= \mathcal{E}_{20} e^{\gamma(x-d)}, \end{aligned}$$

where  $\mathcal{E}_{i0}$  are the amplitudes of the electric field and  $\gamma$  is the damping factor. The solution of 5.2 can be written as

$$C(\lambda) = C \frac{1}{\lambda} \exp \left[ -\gamma_0 \frac{n(\lambda)}{\lambda} \right],$$

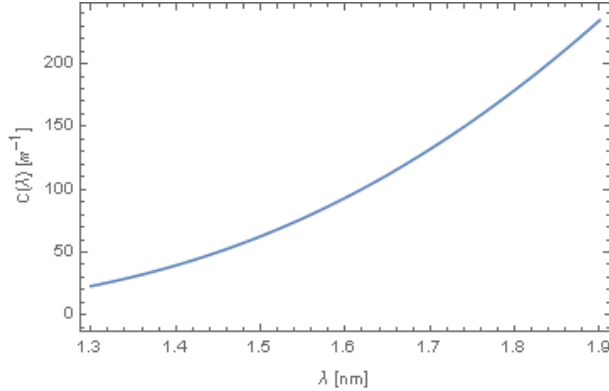


Figure 5.2: The plot of the coupling constant  $C(\lambda)$  for values  $\mathcal{C} = 13 \cdot 10^{-2}$ ,  $\gamma_0 = 4.9 \cdot 10^{-6}$  m.

where we have expected the damping factor dependency as  $\gamma \propto n(\lambda)/\lambda$ . The constant  $\mathcal{C}$  depends on the width  $w$  of the waveguides, on their profiles and on the refractive index difference between the waveguide and substrate and constant  $\gamma_0$  depends on the distance between the waveguides and their mode profiles. We used the values  $\mathcal{C} = 13 \cdot 10^{-2}$  and  $\gamma_0 = 4.9 \cdot 10^{-6}$  m. The plot for these values is on Figure 5.2.

We have set the cut-offs  $M = 34$ ,  $N = 10$ , meaning that we are manipulating with the square matrix  $D$ , given by (4.39), of the order 690.

## 5.2 Calculated Modes

In this section, we present three cases used for the decomposition given by (4.44). Comparison of these model cases shows the dependency of the Schmidt modes on the input parameters.

1. First, we study the degenerate case  $\lambda_s = \lambda_i = 1550.00$  nm with single-channel pump  $A_0 = 1$ . The plots of calculated Schmidt modes are on Figure 5.3. We can see that the adjoint modes seem identical, as would be expected due to the interchangeability of the photons. The Schmidt number has value  $K = 2.32$ .
2. Next case is focused on photon pair with different frequencies (see Figure 5.4). We have selected  $\lambda_s = 1550.00$  nm and  $\lambda_i = 1603.45$  nm. As in the previous case, we assume the single-channel pump  $A_0 = 1$ . We can identify clear differences between the signal and idler modes which are consequence of different values of propagation constants  $C_s$ ,  $C_i$  and coefficients  $b_s$ ,  $b_i$  for different wavelengths of the generated photons. We can also see that the modes are not symmetric with respect to the axis  $k^\perp = 0$ , unlike the previous case. The Schmidt number is  $K = 1.50441$ .

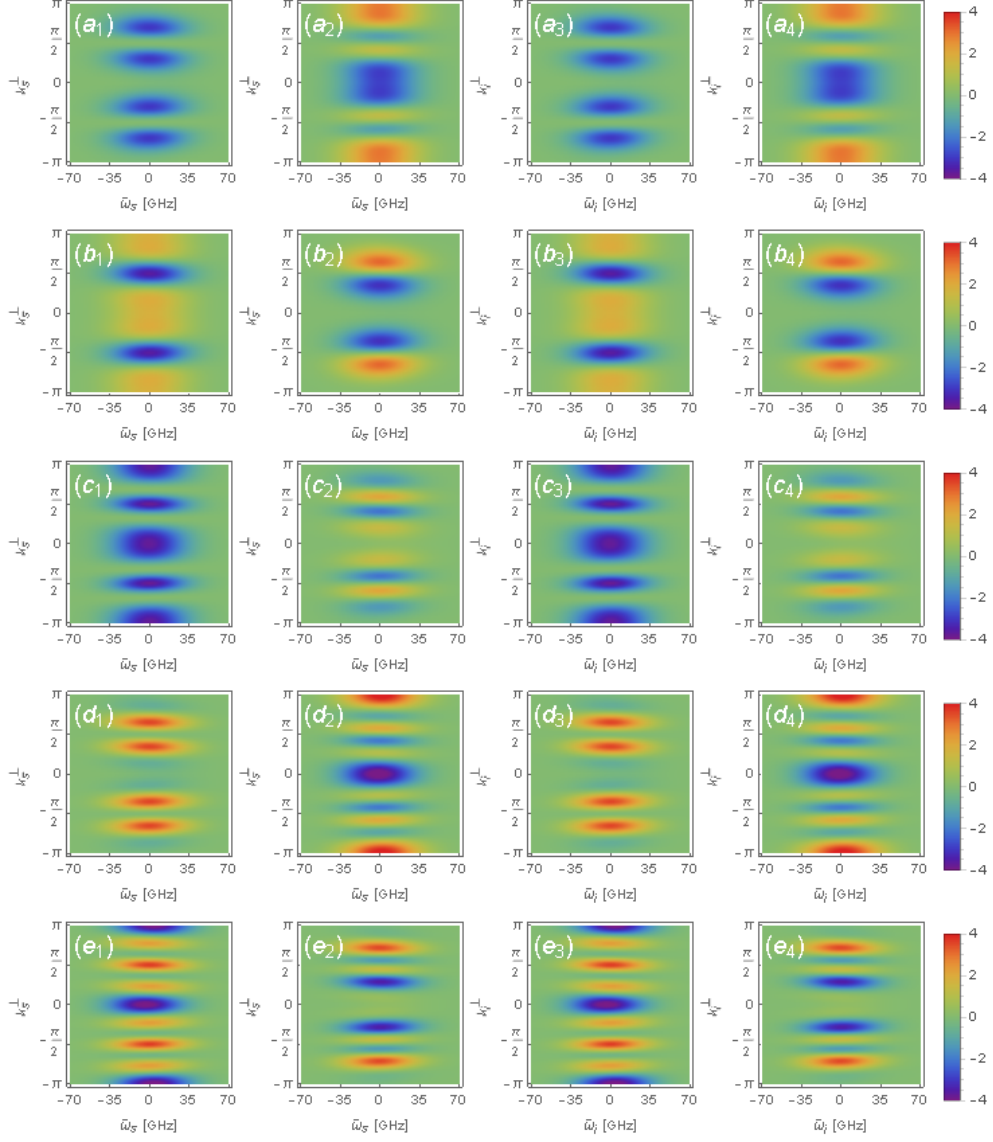


Figure 5.3: The first five adjoint Schmidt modes computed for the degenerate biphoton state at wavelengths  $\lambda_s = \lambda_i = 1550.00$  nm and single-channel pump ( $A_0 = 1$ ). From top to bottom: adjoint Schmidt modes of different orders ( $g_0(\tilde{\omega}_s, k_s^\perp)$ ,  $h_0(\tilde{\omega}_i, k_i^\perp)$ ) in row (a),  $g_2(\tilde{\omega}_s, k_s^\perp)$ ,  $h_2(\tilde{\omega}_i, k_i^\perp)$  in row (b), and so on). From left to right: real and imaginary parts of signal and idler modes (real (1) and imaginary (2) parts of the signal modes in the first two columns and real (3) and imaginary (4) parts of the idler modes in the second ones).

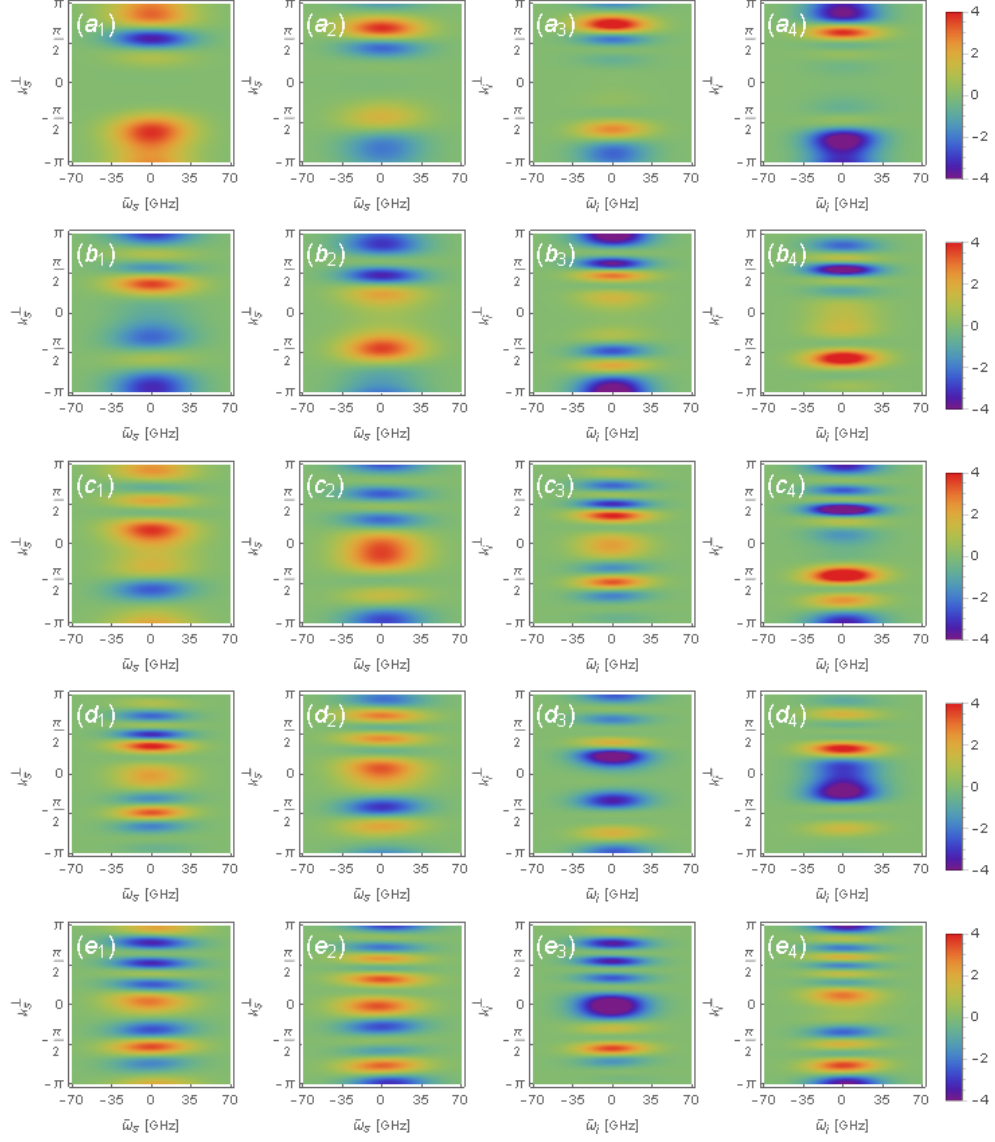


Figure 5.4: The first five adjoint Schmidt modes computed for the biphoton state at wavelengths  $\lambda_s = 1500.00$  nm,  $\lambda_i = 1603.45$  nm and single-channel pump ( $A_0 = 1$ ). From top to bottom: adjoint Schmidt modes of different orders ( $g_0(\tilde{\omega}_s, k_s^\perp)$ ,  $h_0(\tilde{\omega}_i, k_i^\perp)$ ) in row (a),  $g_2(\tilde{\omega}_s, k_s^\perp)$ ,  $h_2(\tilde{\omega}_i, k_i^\perp)$  in row (b), and so on). From left to right: real and imaginary parts of signal and idler modes (real (1) and imaginary (2) parts of the signal modes in the first two columns and real (3) and imaginary (4) parts of the idler modes in the second ones).

3. The last case deals with the degenerate case again, but we suppose two-channel pump  $A_0 = 1$ ,  $A_1=1$  (i.e. the channels  $n = 0$  and  $n = 1$  are illuminated with the same amplitude and phase). The Schmidt modes are plotted on Figure 5.5. It is obvious that the modes are more sharply pronounced, compared to the single-channel pump. The symmetry in the momentum space is violated again. We can see the interplay between the adjoint signal and idler modes when the idler modes seem as signal ones flipped with respect to the axis  $k^\perp = 0$ . It can be expected that this fact is related to the so-called anti-bunching, when the generated photons are detected in opposite waveguides. The Schmidt number is  $K = 4.40$ , meaning that state is the most entangled of the studied ones.

We have seen that the Schmidt modes are clearly dependent on the wavelength of the generated photons and on the parameters characterizing the pump field. On the other hand, the modes for smaller values of detuning from the degeneracy (10 nm for instance) seem to be identical as the ones in the degenerate case (this fact led us to select sufficiently great detuning in the second model case). The two-channel pumping results in sharper modes and higher amount of entanglement.

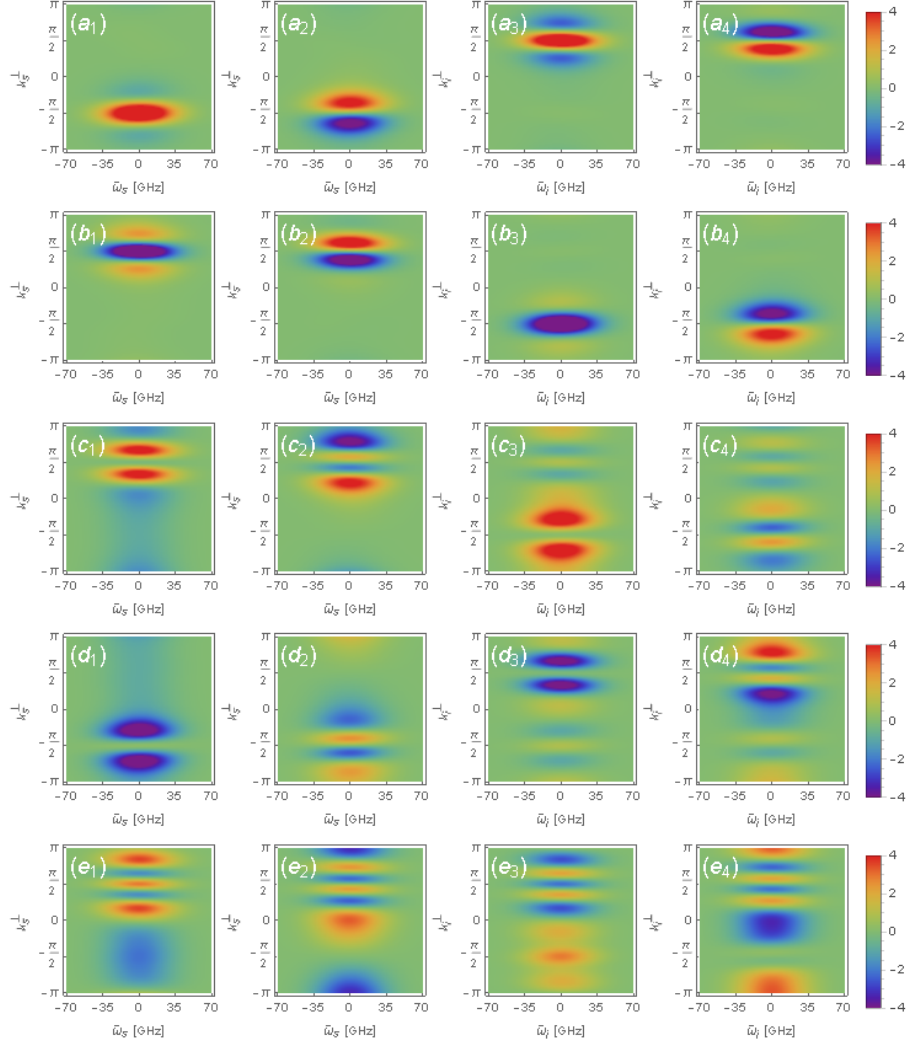


Figure 5.5: The first five adjoint Schmidt modes computed for the biphoton state at wavelengths  $\lambda_s = 1550.00$  nm,  $\lambda_i = 1550.00$  nm and two-channel pump ( $A_0 = 1$ ,  $A_1 = 1$ ). From top to bottom: adjoint Schmidt modes of different orders ( $g_0(\tilde{\omega}_s, k_s^\perp)$ ,  $h_0(\tilde{\omega}_i, k_i^\perp)$  in row (a),  $g_2(\tilde{\omega}_s, k_s^\perp)$ ,  $h_2(\tilde{\omega}_i, k_i^\perp)$  in row (b), and so on). From left to right: real and imaginary parts of signal and idler modes (real (1) and imaginary (2) parts of the signal modes in the first two columns and real (3) and imaginary (4) parts of the idler modes in the second ones).

# Summary

This work is focused on the theoretical examination of the spontaneous parametric down-conversion in waveguide arrays. This quantum process provides us with quantum entangled photon pairs. As we have mentioned before, quantum entanglement is essential for some applications of quantum mechanics. The strength of quantum computation is based on this phenomenon, as well as quantum cryptography. Some quantum algorithms enable us to solve some classically unsolvable tasks and quantum key distribution allows (at least in principle) unbreakable encrypted communication.

In the first chapter, we have outlined the mathematical description of processes in non-linear optics. After the definition of the non-linear susceptibility tensor, we have derived the equations of motion for the electric field in a non-linear medium, starting with the Maxwell's equations. We have derived the coupled equations, providing the classical description of various processes involving the second-order non-linearity. Then, we have introduced the quantum description of spontaneous parametric down-conversion.

The second chapter deals with the description of spontaneous parametric down-conversion in an waveguide array. First, the coupled mode theory is introduced. It describes the propagation of electromagnetic field in the waveguide array, employing some approximations, such as Fresnel approximation and the nearest-neighbour approximation. The dispersion relation, resulting from derived equations of motion, is then used to calculate the output state of down-conversion in the array of waveguides.

In the next chapter, we have recalled the definition of quantum entanglement and we have mentioned some of its measures. We have also introduced the Schmidt decomposition.

In the two last chapters, we are finally dealing with the Schmidt decomposition of the spontaneous parametric down-conversion. First, we show the analytical decomposition of the process in the bulk crystal. For the case of waveguide array, we use the numerical method. The phase-matching function is decomposed with respect to the trigonometric basis and the orthonormal basis consisting of Hermite-Gaussian polynomials. We calculate finite number of Fourier coefficients and then we cut-off the decomposition, assuming sufficient decrease of proportion of higher modes. The resulting matrix is decomposed, using the singular value decomposition, and this allows us to find

the Schmidt coefficients and Schmidt modes.

We have calculated the Schmidt modes for three model cases, presented in the last chapter. Individual cases differed in wavelengths of the generated photons and in the illumination patterns of the incident field. We have seen that both of these conditions affect the shape of Schmidt modes and amount of entanglement. The Schmidt modes therefore can be used to characterize the output biphoton states in the spatio-spectral domain.

The results of this work could serve as a base for further study and they could be utilized in experiments. If we could perform quantum measurements in the Schmidt basis, we would be able to determine the state of the whole system, performing the measurement just on one part of the system – we would know with certainty that the second part would be in the state described by the Schmidt mode adjoint to the measured one. The further theoretical study could generalize the decomposition, involving another configurations (for instance, there are experiments with two-dimensional arrays of waveguides).

# Bibliography

- <sup>1</sup>P. Fiala and I. Richter, *Nelineární optika* (Česká technika - nakladatelství ČVUT, Praha, 2009).
- <sup>2</sup>Wikipedia, *Spontaneous parametric down-conversion* — *Wikipedia, the free encyclopedia*, [Online; accessed 15-June-2015], 2015.
- <sup>3</sup>J. Peřina, *Quantum statistics of linear and nonlinear optical phenomena* (D. Reidel Publishing Company, 1984).
- <sup>4</sup>R. W. Boyd, *Nonlinear optics, third edition* (Academic Press, 2008).
- <sup>5</sup>E. Halenková, A. Černoch, and J. Soubusta, *Spontánní sestupná frekvenční parametrická konverze a zdroj fotonových párů podle návrhu P.G. Kwiat* (Univerzita Palackého v Olomouci, Olomouc, 2012).
- <sup>6</sup>Z. Y. Ou, L. J. Wang, and L. Mandel, “Vacuum effects on interference in two-photon down conversion”, *Phys. Rev. A* **40**, 1428–1435 (1989) [10.1103/PhysRevA.40.1428](#).
- <sup>7</sup>C. K. Hong and L. Mandel, “Theory of parametric frequency down conversion of light”, *Phys. Rev. A* **31**, 2409–2418 (1985) [10.1103/PhysRevA.31.2409](#).
- <sup>8</sup>S. Walborn, C. Monken, S. Padua, and P. S. Ribeiro, “Spatial correlations in parametric down-conversion”, *Physics Reports* **495**, 87–139 (2010) [10.1016/j.physrep.2010.06.003](#).
- <sup>9</sup>C. H. Monken, P. H. S. Ribeiro, and S. Padua, “Transfer of angular spectrum and image formation in spontaneous parametric down-conversion”, *Phys. Rev. A* **57**, 3123–3126 (1998) [10.1103/PhysRevA.57.3123](#).
- <sup>10</sup>J. Schneeloch and J. C. Howell, “Introduction to the transverse spatial correlations in spontaneous parametric down-conversion through the biphoton birth zone”, *Journal of Optics* **18**, 053501 (2016) [10.1088/2040-8978/18/5/053501](#).
- <sup>11</sup>M. Bellec, G. M. Nikolopoulos, and S. Tzortzakis, “Quantum state transfer and network engineering”, in , edited by M. G. Nikolopoulos and I. Jex (Springer Berlin Heidelberg, Berlin, Heidelberg, 2014) Chap. State Transfer Hamiltonians in Photonic Lattices, pp. 223–245, [10.1007/978-3-642-39937-4\\_7](#).

- <sup>12</sup>H. Trompeter, “Discrete optics in inhomogeneous waveguide arrays”, PhD thesis (Friedrich-Schiller Universität Jena, 2006).
- <sup>13</sup>F. Lederer, G. I. Stegeman, D. N. Christodoulides, G. Assanto, M. Segev, and Y. Silberberg, “Discrete solitons in optics”, *Physics Reports* **463**, 1–126 (2008) 10.1016/j.physrep.2008.04.004.
- <sup>14</sup>R. Kruse, F. Katzschmann, A. Christ, A. Schreiber, S. Wilhelm, K. Laiho, A. Gábris, C. S. Hamilton, I. Jex, and C. Silberhorn, “Spatio-spectral characteristics of parametric down-conversion in waveguide arrays”, *New Journal of Physics* **15**, 083046 (2013) 10.1088/1367-2630/15/8/083046.
- <sup>15</sup>A. S. Solntsev, A. A. Sukhorukov, D. N. Neshev, and Y. S. Kivshar, “Spontaneous parametric down-conversion and quantum walks in arrays of quadratic nonlinear waveguides”, *Phys. Rev. Lett.* **108**, 023601 (2012) 10.1103/PhysRevLett.108.023601.
- <sup>16</sup>S. M. Barnett and S. J. D. Phoenix, “Entropy as a measure of quantum optical correlation”, *Phys. Rev. A* **40**, 2404–2409 (1989) 10.1103/PhysRevA.40.2404.
- <sup>17</sup>M. A. Nielsen and I. L. Chuang, *Quantum computation and quantum information*, Cambridge Books Online (Cambridge University Press, 2010), 10.1017/CB09780511976667.
- <sup>18</sup>I. Bengtsson and K. Życzkowski, *Geometry of quantum states*, Cambridge Books Online (Cambridge University Press, 2006), 10.1017/CB09780511535048.
- <sup>19</sup>J. Blank, P. Exner, and M. Havlíček, *Lineární operátory v kvantové fyzice* (Karolinum, Praha, 1993).
- <sup>20</sup>J. Liesen and V. Mehrmann, *Linear algebra* (Springer International Publishing, 2015), 10.1007/978-3-319-24346-7.
- <sup>21</sup>E. Schmidt, “Zur Theorie der linearen und nichtlinearen Integralgleichungen”, *Mathematische Annalen* **63**, 433–476 10.1007/BF01449770.
- <sup>22</sup>M. Fedorov and N. Miklin, “Schmidt modes and entanglement”, *Contemporary Physics* **55**, 94–109 (2014) 10.1080/00107514.2013.878554.
- <sup>23</sup>F. Miatto, H. Di Lorenzo Pires, S. Barnett, and M. van Exter, “Spatial Schmidt modes generated in parametric down-conversion”, English, *The European Physical Journal D* **66**, 263 (2012) 10.1140/epjd/e2012-30035-3.
- <sup>24</sup>F. Miatto, T. Brougham, and A. Yao, “Cartesian and polar Schmidt bases for down-converted photons”, English, *The European Physical Journal D* **66**, 183 (2012) 10.1140/epjd/e2012-30063-y.
- <sup>25</sup>E. D. Rainville, *Special functions* (The Macmillan Co., New York, 1960), pp. xii+365.

- <sup>26</sup>M. Abramowitz and I. A. Stegun, *Handbook of Mathematical Functions with Formulas, Graphs and Mathematical Tables* (Dover Publications, New York, 1972).
- <sup>27</sup>G. N. Watson, “Notes on Generating Functions of Polynomials: (1) Laguerre Polynomials”, *Journal of the London Mathematical Society* **s1-8**, 189–192 (1933) [10.1112/jlms/s1-8.3.189](https://doi.org/10.1112/jlms/s1-8.3.189).
- <sup>28</sup>L. Lamata and J. León, “Dealing with entanglement of continuous variables: Schmidt decomposition with discrete sets of orthogonal functions”, *Journal of Optics B: Quantum and Semiclassical Optics* **7**, 224 (2005) [10.1088/1464-4266/7/8/004](https://doi.org/10.1088/1464-4266/7/8/004).
- <sup>29</sup>Wolfram Research, Inc., *Mathematica 10.3*, Champaign, Illinois, 2015.
- <sup>30</sup>A. Cheriguene, H. Bouridah, and M. R. Beghoul, “A novel numerical technique for simultaneous calculations of type II phase matching angle and temperature for second harmonic generation in negative uniaxial crystals”, *Optik - International Journal for Light and Electron Optics* **127**, 3633–3637 (2016) [10.1016/j.ijleo.2015.12.154](https://doi.org/10.1016/j.ijleo.2015.12.154).